

Enrichment of the hot intracluster medium: numerical simulations

V. Biffi · F. Mernier · P. Medvedev

Received: date / Accepted: date

Abstract The distribution of chemical elements in the hot intracluster medium (ICM) retains valuable information about the enrichment and star formation histories of galaxy clusters, and on the feedback and dynamical processes driving the evolution of the cosmic baryons. In the present study we review the progresses made so far in the modelling of the ICM chemical enrichment in a cosmological context, focusing in particular on cosmological hydrodynamical simulations. We will review the key aspects of embedding chemical evolution models into hydrodynamical simulations, with special attention to the crucial assumptions on the initial stellar mass function, stellar lifetimes and metal yields, and to the numerical limitations of the modelling. At a second stage, we will overview the main simulation results obtained in the last decades and compare them to X-ray observations of the ICM enrichment patterns. In particular, we will discuss how state-of-the-art simulations are able to reproduce the observed radial distribution of metals in the ICM, from the core to the outskirts, the chemical diversity depending on cluster thermo-dynamical properties, the evolution of ICM metallicity and its dependency on the system mass

V. Biffi

Physics Department, Astronomy Unit, Trieste University, v. Tiepolo 11, 34143 Trieste (Italy)
INAF, Observatory of Trieste, v. Tiepolo 11, 34143 Trieste (Italy)
E-mail: biffi@oats.inaf.it

F. Mernier

MTA-Eötvös University Lendület Hot Universe Research Group, Pázmány Péter sétány 1/A, Budapest, 1117, Hungary
Institute of Physics, Eötvös University, Pázmány Péter sétány 1/A, Budapest, 1117, Hungary
SRON Netherlands Institute for Space Research, Sorbonnelaan 2, 3584 CA Utrecht, The Netherlands

P. Medvedev

Space Research Institute of the Russian Academy of Sciences (IKI), 84/32 Profsoyuznaya Str, Moscow, 117997, Russia

from group to cluster scales. Finally, we will discuss the limitations still present in modern cosmological, chemical, hydrodynamical simulations and the perspectives for improving the theoretical modelling of the ICM enrichment in galaxy clusters in the future.

Keywords Galaxy Clusters · ICM chemical enrichment · Numerical Simulations

1 Introduction

In the hierarchical paradigm of structure formation, clusters of galaxies are the largest and latest systems formed in the Universe from the gravitational collapse of large overdense regions. Despite a dominating dark matter component ($\sim 85\%$ of the total mass budget), observations of galaxy clusters reveal that a fraction of their content is in the form of stars in galaxies and of a hot diffuse gas, the intra-cluster medium (ICM). Filling the dark-matter dominated potential wells of galaxy clusters and groups, this hot plasma carries the imprint of the cluster formation and evolution, and the study of its thermodynamical and chemical properties is an invaluable source of information about the star formation and feedback histories.

X-ray observations of the hot ($T \sim 10^7\text{--}10^8$ K) ICM allow us to derive directly its thermal properties (from density and temperature), but have also shown that the ICM spectrum is characterized by emission lines from heavy elements. This indicates that a non-negligible fraction of this gas must have been enriched with heavy ions from stars (principally) within galaxies before it became part of the diffuse ICM component. The abundance and spatial distribution of these metals (namely all the chemical elements heavier than helium) is therefore influenced by several complex physical and dynamical processes that drive the formation and evolution of galaxies and their interaction with the ambient intracluster medium (see Schindler and Diaferio 2008, for a review). From the study of the gas chemical enrichment in local clusters and its evolution with time, we can therefore derive constraints on the main physical processes shaping their observable properties, from the merging and star-formation histories, to the effects of non-gravitational sources of energy like feedback from supernova (SN) winds and Active Galactic Nuclei (AGN).

The metals that enrich the ICM are produced by stars and stellar remnants. In particular, α - and iron-peak elements are mostly synthesized during stellar lifetimes and SN explosions, and are then released into the surrounding gas. Core-collapse supernovae (to which we refer as SNII, in the following), originate from massive short-living stars and primarily produce oxygen (O) and some other α -elements, such as neon (Ne) and magnesium (Mg). Type-Ia supernovae (SNIa), arising from the explosions of white dwarf stars in binary systems, are mostly responsible for the production of heavier elements, especially iron (Fe) and nickel (Ni). Intermediate-mass elements like silicon (Si), sulfur (S), argon (Ar) and calcium (Ca) are mainly released by SNII, whereas the bulk of carbon (C) and nitrogen (N) and neutron-rich isotopes of Ne,

Mg, as well as Na, Al are produced and ejected by low- and intermediate-mass stars during the asymptotic giant branch (AGB) phase (e.g. Böhringer and Werner 2010; Nomoto et al. 2013; de Plaa 2013; Karakas and Lattanzio 2014). Despite this picture is fairly well established, several uncertainties still remain, especially in the details of stellar evolution models for SN. Thus, useful constraints on the various models can be derived from measurements of abundance patterns of different elements in the intracluster gas, and from differences with respect to the theoretical model predictions (see Mernier et al., *subm.*, this issue, for a recent detailed review on chemical measurements from X-ray data).

Other than observations of the metal abundances in the ICM, theoretical investigations by means of numerical simulations are extremely powerful to explore the enrichment history of the gas. In fact, cosmological hydrodynamical simulations uniquely allow to simultaneously follow a large variety of highly non-linear, complex physical processes driving the co-evolution of dark matter and baryonic matter in the Universe. In particular, state-of-the-art simulations can account for detailed treatments of the most important gas-dynamical processes that shape the properties of galaxy clusters during their formation and evolution: from gas cooling and star formation, to stellar evolution and consequent production of chemical elements, including stellar and AGN feedback processes. Therefore, they can be exploited to investigate the details of the ICM chemical properties at different epochs, the expected signatures of energy feedback processes on the distribution of metals, and the relation between the distribution of chemical elements in the ICM and the cluster formation and evolution. Moreover, simulations can be used to study the connection between different enrichment patterns of the ICM and the resulting thermal structure and star formation history of galaxy clusters, given that metals alter the gas cooling through their several cooling lines.

Since the late 90s, several groups started to couple chemical evolution models with hydrodynamical simulations of galaxies (Raiteri et al. 1996; Mosconi et al. 2001), and of galaxy clusters (Lia et al. 2002; Kawata and Gibson 2003; Valdarnini 2003; Tornatore et al. 2004; Scannapieco et al. 2005; Tornatore et al. 2007; Davé et al. 2008; Wiersma et al. 2009b). In the past 15 years, advancements in the modelling of the chemical properties have also been accompanied by substantial improvements in the description of the various physical processes driving the evolution of the baryonic component, such as energy feedback from stellar and AGN sources (Springel et al. 2005; Di Matteo et al. 2005; Scannapieco et al. 2005; Sijacki and Springel 2006; Fabjan et al. 2010; Teyssier et al. 2011; Dubois et al. 2011; Planelles et al. 2014; Martizzi et al. 2016; Barnes et al. 2017). Despite some limitations still persist (e.g. on the details of the baryonic cycle in cluster cores and of the feedback scheme), cluster simulations have reached an unprecedented level of detail. Recent simulation campaigns carried on by different groups have in fact succeeded in reproducing more realistic cluster properties, for instance recovering the observed thermal and chemical diversity of cool-core and non-cool-core clusters (Rasia et al. 2015; Hahn et al. 2015; Martizzi et al. 2016; Biffi et al. 2017; Barnes et al.

2018; Vogelsberger et al. 2018). Although not discussed in this paper, theoretical investigations of the chemical enrichment of the inter-galactic gas in clusters and groups have also been pursued via semi-analytical techniques, coupling DM-only or non-radiative simulations with semi-analytical models of galaxy formation and evolution that account, with various level of detail, for the chemical enrichment processes from SN explosions and AGB stars in galaxies. Several of these works, explored the spatial distribution of metals in the ICM and the impact of the various physical and dynamical processes onto the final cluster enrichment level (De Lucia et al. 2004; Nagashima et al. 2005; Schindler et al. 2005; Domainko et al. 2006; Cora 2006; Cora et al. 2008; Moll et al. 2007; Kapferer et al. 2007; Short et al. 2013; Yates et al. 2017).

With respect to the review by Borgani et al. (2008) on ICM chemical enrichment in simulated clusters, important improvements have been obtained from the numerical side. Most of all, the difficulties of regulating overcooling at the cluster center while reproducing the thermodynamical diversity of observed cool-core and non-cool-core systems have been overcome in the past five years, as discussed above. This allowed different independent groups to obtain more and more realistic simulations of galaxy clusters, in which to explore more faithfully the details of the ICM chemo-dynamical history. Therefore, we review in this article the latest and most important results on the chemical enrichment of the ICM, focusing on state-of-the-art numerical hydrodynamical simulations in a cosmological context.

In particular, the paper is structured as follows. In Sec. 2 we outline the building blocks of chemical evolution models and overview the progresses made so far to include them into cosmological hydrodynamical simulations (Sec. 2.1). In Sec. 3 we summarize the most important simulation results on the modelling of the distribution of chemical elements in the ICM, from the centermost regions out to the outskirts, while its evolution with time is discussed in Sec. 4. The dependence of the chemical enrichment on the system scale, from groups to clusters of galaxies, is then reviewed in Sec. 5. Finally, we conclude by overviewing the principal limitations that are still present in modern cosmological chemo- and hydro-dynamical simulations (Sec. 6).

As such, this article complements the review by Mernier et al. 2018 (subm., this issue), where the most significant achievements in measuring the ICM chemical properties from X-ray observations are reviewed.

2 Chemical evolution models in simulations

In this section, we provide a brief description of the basic structure and features of chemical evolution models implemented in numerical simulations (e.g., see also Borgani et al. 2008). Including these models in simulations of galaxies and clusters is of great importance because the metal-rich ejecta from evolved stellar populations determine the heavy-element content of the inter-galactic and intra-cluster gas.

Cosmological hydrodynamical simulations of large volumes, even in the case of *zoom-in* re-simulations of galaxies or galaxy clusters, cannot reach the resolution needed to resolve single stars and must therefore resort to sub-grid models of star formation and chemical enrichment. Typically, star formation is described by the conversion of a gas element into a “star” element, as a consequence of the cooling of the gas. This approach was adopted, for instance, in the first implementation of star formation in SPH simulations by Katz (1992), and later in the effective models for multi-phase inter-stellar medium description presented by Springel and Hernquist (2003) or by Murante et al. (2010). Given the typical resolution of large-scale simulations, the star element has a mass of $10^4\text{--}10^6 h^{-1} M_{\odot}$ and rather represents a population of stars, all with the same age and initial metallicity, i.e. a simple stellar population (SSP), characterized by an assumed initial mass function (IMF). For every star element in the simulation one can compute the evolution of the stellar population that it represents, by assuming not only the IMF, but also some mass-dependent lifetime function and stellar yields associated to the various mass ranges and enrichment channels.

Briefly, we recall hereafter these pillars of chemical evolution models embedded into cosmological hydrodynamical simulations.

Ejection channels of heavy elements

The chemical feedback in simulations typically originates from three main stellar evolution channels: SNII, SNIa, and stars undergoing the AGB phase (e.g. Tornatore et al. 2004, 2007; Davé et al. 2008; Wiersma et al. 2009b).

The calculations constituting the core of chemical evolution models are a set of integral equations. These compute the rates at which stars of different masses explode as SNII, SNIa or undergo the AGB phase in each SSP and the corresponding metal ejecta that will enrich the surrounding gas (we refer the reader to Matteucci 2003, for a more detailed description).

Stellar yields

Stellar yields from stellar evolution models provide the amount of different metal species released during the evolution of a SSP. This quantity depends on the star initial mass and metallicity. Many groups in the past decades have calculated and proposed various sets of stellar yields for massive, intermediate- and low-mass stars. In the literature, the most widely used in hydrodynamical simulations embedding chemical enrichment models are those by Woosley and Weaver (1995), Portinari et al. (1998), Chieffi and Limongi (2004) and Kobayashi et al. (2006) for SNII; the sets proposed by Nomoto et al. (1997), Iwamoto et al. (1999), Thielemann et al. (2003) and Travaglio et al. (2004) for SNIa; and for low- and intermediate-mass stars the tables by van den Hoek and Groenewegen (1997), Marigo (2001), Karakas and Lattanzio (2007), Karakas (2010) and Doherty et al. (2014) (see also Karakas and Lattanzio 2014, for further references of AGB yields sets available in the literature).

Unfortunately, yields for many elements (especially the iron-peak ones) can actually vary significantly, by up to some order of magnitudes, from author to author. The choice of the set of yields that is included as an input parameter in the simulations inevitably affects the final predictions from theoretical models. In fact, this still represents an important source of uncertainties in predicting the precise chemical enrichment level of the inter-stellar medium and ICM derived from cosmological hydrodynamical simulations.

Lifetime function

In order to describe the evolution of a SSP and the enrichment channels through which the stellar population produces and releases metals, it is crucial to know the typical lifetimes of stars with different masses. Various functional forms for the mass-dependence of the lifetimes have been proposed in the literature. The most commonly adopted ones in simulations are those by Maeder and Meynet (1989), Padovani and Matteucci (1993), and Chiappini et al. (1997), among which the main differences concern the lifetimes of low-mass stars. Typically, the lifetimes are a decreasing function of the stellar mass. With respect to the enrichment channels considered in simulations, we note therefore that SNIa and AGB sources are typically related to the evolution of low- and intermediate-mass stars with longer lifetimes, whereas viceversa SNII events originate from massive short-living stars.

In the majority of the cases the above-mentioned mass-dependent lifetime functions are adopted. We recall nonetheless that the stellar lifetimes can also depend on metallicity, like those presented by Portinari et al. (1998) (see also Romano et al. 2005, for an overview and differences between various functional forms in the literature).

Initial mass function (IMF)

Another key ingredient of chemical models is the IMF, namely a functional form that parametrizes the number of stars as a function of their mass. Its shape essentially constrains the relative ratio between low-mass long-living stars and massive short-living ones (e.g., Romano et al. 2005). The choice of the IMF function has profound impact on the modelling of metal enrichment since it is directly connected to the relative abundance of SNIa and SNII, and consequently to the abundance ratios of elements produced by the two different channels (i.e. α vs. Fe-peak elements). Other than chemical feedback, also the modelling of the stellar energy feedback, associated to SNII-driven winds, will be affected by the relative fractions of stars with different masses and specifically to the abundance of massive stars.

Historically, the most commonly adopted IMF is the one introduced by Salpeter (1955), which is characterized by a single power-law shape, $\phi(m) \propto m^{-\alpha}$, with a (logarithmic) slope of $\alpha = 1.35$. Arimoto and Yoshii (1987) also proposed a single power-law IMF but with a shallower slope,

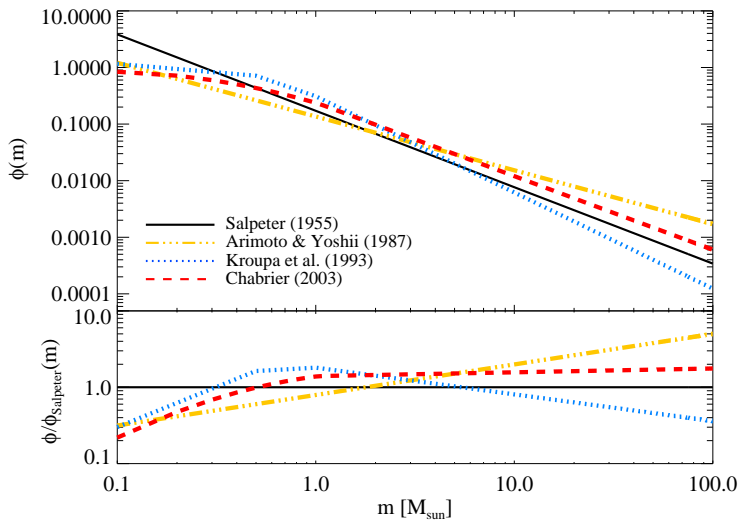


Fig. 1 Comparison between different stellar IMFs. As an example we show the single power-law IMF functions by Salpeter (1955) and Arimoto and Yoshii (1987), the multi-slope power-law IMF by Kroupa et al. (1993), and the IMF proposed by Chabrier (2003) with its lognormal shape at low stellar masses.

$\alpha = 0.95$, that predicts a larger number of massive stars compared to the Salpeter IMF. IMF functions of this sort are typically referred to as top-heavy.

Other IMF functions, also widely used in the literature, allow for a change of the IMF accordingly to the mass. This is the case for the Kroupa IMF (Kroupa et al. 1993; Kroupa 2001) and the Chabrier IMF (Chabrier 2003). The former is essentially parametrized by a multi-slope power-law form, whereas the Chabrier IMF is characterized by a power law at high stellar masses and by a log-normal form (first introduced by Miller and Scalo 1979) at the lower-mass end. The changes to the single-slope Salpeter IMF were developed starting from the late 1970s in order to reproduce the shallower IMF towards the low stellar masses indicated by a number of observational constraints.

The impact of changing the IMF on the fraction of stars in the various mass bins can be seen for instance in Fig. 1, where we compare directly the IMFs by Salpeter (1955) ($\phi(m) \propto m^{-1.35}$), Arimoto and Yoshii (1987) ($\phi(m) \propto m^{-0.95}$), Kroupa et al. (1993) (with 3 slopes: $\alpha = 0.3$ for $m < 0.5 M_{\odot}$, $\alpha = 1.2$ for $0.5 < m/M_{\odot} < 1$ and $\alpha = 1.7$ for $m > 1 M_{\odot}$), and Chabrier (2003) (with a power-law slope of $\alpha = 1.3$ in the $m > 1 M_{\odot}$ regime, and $\phi(m) \propto \exp(-(\log(m) - \log(m_c))^2/2\sigma^2)$ with $m_c = 0.079$ and $\sigma = 0.69$ for $m < 1 M_{\odot}$). In the top panel we show the four functional forms as a function of mass and in the lower panel we report the ratio with respect to the Salpeter IMF. All the reported IMFs are normalized between 0.1 and $100 M_{\odot}$.

The universality of the IMF is actually still matter of debate (see Bastian et al. 2010, for a review on IMF variations), with a number of works exploring the possibility of an IMF functional form that changes with galaxy environment and morphology (see, e.g. Bernardi et al. 2018, and references therein), as well as with time.

2.1 Embedding chemical models into hydrodynamical simulations

Cosmological hydrodynamical simulations including the treatment of chemistry have been developed by several groups in the last couple of decades, starting with the early works by Raiteri et al. (1996), Lia et al. (2002) and Kawata and Gibson (2003) on galaxies, comprising Milky-Way-like objects and ellipticals, also in a cosmological context as in Steinmetz and Mueller (1994) and Mosconi et al. (2001).

Simulations of galaxy clusters and larger cosmological volumes also started to include models of chemical evolution since the early 2000s. Valdarnini (2003) presented results on the iron profiles of a set of galaxy clusters obtained with an SPH set of cosmological chemical hydrodynamical simulations. In that work, the enrichment from SNIa and SNII was considered, together with a metallicity-dependent cooling function. In the paper the author discusses the effects on the ICM iron profiles depending on the numerical resolution and on model parameters (IMF, metal ejection profile and diffusion length). Later, the first implementations of chemical evolution modules were included into the GADGET-2 code (Springel 2005), that is still one of the most commonly used SPH codes for cosmological simulations. These implementations only included metal production from SNII under the assumption of instantaneous recycling approximation and no metallicity dependence of the cooling function. Scannapieco et al. (2005) presented results on the enrichment in simulated galaxies by adopting a chemical model in GADGET-2 that included star formation, cooling, feedback and metal enrichment from SNIa and SNII. Tornatore et al. (2004, 2007) presented a more detailed implementation of the chemical evolution model into GADGET-2, which comprises a refined treatment for metallicity-dependent cooling, metallicity-dependent yields and included the enrichment due to intermediate- and low-mass stars undergoing the AGB phase (see also Davé et al. 2008). Wiersma et al. (2009b,a) also presented chemical hydrodynamical simulations performed with the SPH code GADGET-2, where they instead adopted metallicity-dependent lifetimes by Portinari et al. (1998). In the 2000s, other groups working with different SPH codes also started to include detailed models for chemical evolution in simulations of galaxy clusters. For instance, Romeo et al. (2006) presented zoomed re-simulations of galaxy clusters performed with the TREESPH code by Sommer-Larsen et al. (2003), including chemical evolution with non-instantaneous recycling of gas and heavy elements (based on the model by Lia et al. (2002)), in addition to metal-dependent cooling, star formation, feedback from starburst-driven galactic winds and thermal conduction.

More recently, advanced cosmological hydrodynamical simulations performed with various codes, both SPH and grid-based, have combined chemical models with several other physical processes, including feedback from stellar and active galactic nuclei (AGN) sources, with the purpose of obtaining more realistic simulations of galaxy clusters that can be compared against the increasingly detailed observational databases available (Sijacki and Springel 2006; Puchwein et al. 2008; Fabjan et al. 2010; Teyssier et al. 2011; Dubois et al. 2011; Planelles et al. 2014; Martizzi et al. 2016; Biffi et al. 2017; Dolag et al. 2017; Barnes et al. 2017; Vogelsberger et al. 2018).

In addition to computing the global metallicity in the gas and stellar components of the simulations, many of the modern chemical hydrodynamical codes are able to trace individual metal species as well, including not only iron, but also several additional chemical elements, such as oxygen, silicon, calcium, nickel, etc. Moreover, in some simulations, the source of the enrichment is also specifically tracked, which allows to reconstruct how much of the metal budget is produced by each one of the followed enrichment channels, namely SNIa, SNII and AGB (Tornatore et al. 2007; Biffi et al. 2017, 2018; Vogelsberger et al. 2018; Naiman et al. 2018).

2.1.1 Impact of the model assumptions

When dealing with chemical hydrodynamical simulations, there are a number of crucial aspects to take into account. In particular, the choice of the IMF, of the stellar lifetime function and of the set of stellar yields have an ultimate influence on the resulting metal enrichment. The amount of metals, in turn, is crucial because has also an impact on the cooling of the gas — which has a strong dependence on metallicity (e.g. Sutherland and Dopita 1993; Maio et al. 2007; Wiersma et al. 2009a) — and consequently on the history of star formation.

The effects of varying the assumed IMF or the set of stellar yields can be significant. As we mentioned in the previous sections, different IMFs provide different relative ratios of low-mass and high-mass stars, which reflects into different abundance ratios. For instance, Romeo et al. (2006) presented an analysis on the effects of varying the IMF on the ICM enrichment in simulations of galaxy clusters, showing that in simulations where an efficient feedback mechanism is not present and iron abundance profiles result to be too steep compared to observed ones, adopting a top-heavier IMF rather than a Salpeter IMF can alleviate the discrepancy. Similarly, Tornatore et al. (2007) found that changing the IMF, among the various model assumptions, has the strongest impact on the resulting metal enrichment of the ICM. In particular they showed that assuming a top-heavier IMF (such as the one proposed by Arimoto and Yoshii 1987) with respect to the Salpeter one turns into an increase of the ICM iron metallicity by a factor of two and that of oxygen by a factor of three, with a consequent increase of the oxygen-over-iron abundance ratio. The authors also showed that the assumption of the multi-slope Kroupa IMF (Kroupa 2001), on the contrary, results into a decrease of the O/Fe abundance ratio with re-

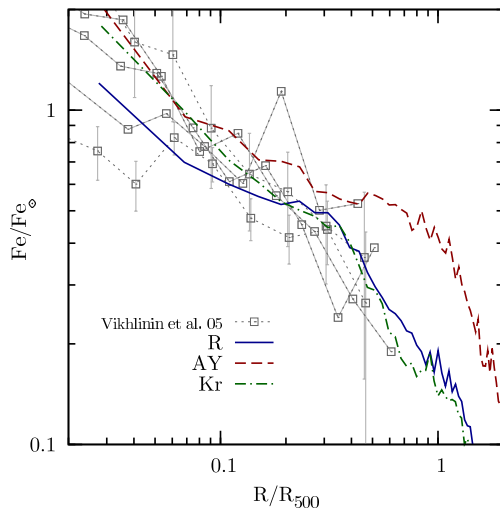


Fig. 2 Effects of changing the IMF on the resulting Fe abundance profile; taken from Tornatore et al. (2007). Simulated Fe profiles assuming the IMF by Salpeter (R; blue solid line), Kroupa (Kr; green dot-dashed line) and Arimoto and Yoshii (1987) (AY; red dashed line) are compared against observational data by Vikhlinin et al. (2005) (grey symbols). Iron abundances are rescaled with respect to the reference solar values by Anders and Grevesse (1989).

spect to a Salpeter IMF, due to a smaller number of massive stars. In this case, however, the Fe abundance profile is very similar to the Salpeter one, at large cluster-centric distances ($r \gtrsim 0.2 R_{500}$). These results by Tornatore et al. (2007) on the Fe radial profile, for the three simulation runs obtained for the IMF by Salpeter (1955), Kroupa (2001) and Arimoto and Yoshii (1987), are reported in Fig. 2.

Given the sensitivity of element abundance ratios to the relative distribution of different types of SNe and AGB stars, not only the proportion given by the IMF is important but also the different time scales contribute to different signatures in the final enrichment. The most important effect of changing the lifetime functions, however, is on the enrichment history, post-poning or anticipating the typical epoch of ICM enrichment.

The amount of metals produced, and the relative abundances of different elements, in simulations also depends directly on the set of stellar yields adopted. Given the uncertainties thereto related, simulation analyses that investigate the chemical content of clusters and galaxies should always clearly specify the sets of yields used, given the uncertainties thereto related. In fact, as shown by Wiersma et al. (2009b), the predictions of different sets of yields can differ by factors of a few in the ejected masses of individual elements released by AGB and SNII, which translates into uncertainties by a factor of a few in the elemental ratios, for a fixed IMF. The effects of these differences onto the final ICM enrichment is however not straightforward, given that the metal production depends in a non-trivial way on the SSP characteristics, such as its initial metallicity, which depends in turn on several factors (epoch of formation, star

formation history etc.). For instance, Tornatore et al. (2007) showed that using the sets of SNII yields by either Woosley and Weaver (1995) or Chieffi and Limongi (2004), despite their different element production, produce relatively similar Fe abundance and O/Fe ratio profiles.

Degeneracies in the model assumptions can alone alter the ICM final chemical pattern, especially — but not only — in the level of the enrichment. Because of these degeneracies, the choice of IMF, lifetime function and yield tables is therefore a delicate aspect. In Vogelsberger et al. (2018), for instance, the authors describe how changing the details of their chemical evolution model from Illustris to IllustrisTNG, with significant updates of the SNII yield tables and of the SNIa rates, can ultimately cause sizeable differences in the integrated metal production over one Hubble time, namely by up to a factor of ~ 2 in the case of iron. Nonetheless, we also remind that other crucial physical processes, above all energy feedback, interplay in a complex way with the chemical model, and simulations must at the same time reproduce both thermo- and chemo-dynamical properties of the ICM, and possibly properties of the cluster galaxy population, in order to be successful.

2.1.2 Numerical limitations

Also the details of the chemical model implemented included in the simulations and the numerical resolution can impact the resulting chemical enrichment of the ICM.

Unfortunately, an accurate treatment of gas mixing within large-scale simulations is challenging, given the difficulty in following the development of turbulence and mixing even when the small scales involved are resolved. Eulerian hydrodynamical codes implicitly include some numerical diffusion, which can produce mixing that depends on the specific implementation adopted and is often strong (e.g. Springel 2010). Differently, Lagrangian methods such as SPH require the implementation of an explicit mixing scheme, for instance adopting a diffusion model. Greif et al. (2009) proposed a method of chemical mixing in SPH simulations that is based on the velocity dispersion within the SPH smoothing kernel. Although applied to the evolution of a supernova remnant, this algorithm is quite generic and can be suitable for simulations of the chemical enrichment of the interstellar and intergalactic medium. Recently, Williamson et al. (2016) presented a series of SPH simulations of isolated galaxies performed with the N -body/smoothed-particle-chemodynamics code GCD+ (Kawata et al. 2014, and references therein), including also chemical enrichment with a metal diffusion algorithm based on the method by Greif et al. (2009). By comparing different metal mixing schemes, the authors show that, depending on the diffusion strength, the metals can flow out of the galactic disk without any resolved mass flow or rather be retained and transported by galactic outflows. This has therefore a critical impact on determining the dominant processes in place in a galaxy, and can in turn influence their chemical feedback to the surrounding medium. Despite the few attempts done so far to include the treatment of diffusion processes in SPH simulations, we remind that these

have been typically limited to the scale of the smoothing kernel. Nonetheless, transport mechanisms on larger scales might also play an important role and much more realistic and detailed analyses are still strongly needed.

A frequently adopted approach to modelling chemical mixing in SPH codes, especially for cosmological large-scale simulations, is to assume that the products of stellar nucleosynthesis are distributed within a fixed volume. The distribution of metals from the stellar source onto the surrounding gas elements is typically done by smoothing the metallicities onto neighbour gas particles according to the same SPH kernel used for the computation of the hydrodynamic quantities (e.g. Mosconi et al. 2001). Tests presented by Tornatore et al. (2007) showed that changing the kind of filter function, the number of neighbour gas particles or the weighting scheme used to perform the smoothing has a modest impact on the overall stellar population and ICM enrichment in simulated clusters. The differences introduced by these choices are typically smaller than the cluster-to-cluster variations. Valdarnini (2003) also explored the variations on the ICM iron profiles due to changes in the model parameters of the metal ejection scheme, for a given IMF, and found changes by a factor of 1–2 in the normalization of the resulting iron radial distribution.

Another crucial aspect is the impact of numerical resolution on the predictions from simulations on the ICM enrichment, as discussed in several works in the literature (e.g. Valdarnini 2003; Tornatore et al. 2007; Wiersma et al. 2009a; Martizzi et al. 2016; Vogelsberger et al. 2018). In the early investigations by Valdarnini (2003), cluster simulations with increased numerical resolution provided generally consistent iron abundance profiles with respect to the low-resolution reference runs.

Later numerical analyses indicated instead as a general finding that the level of enrichment of the ICM tends to increase at higher resolution. Tornatore et al. (2007), for instance, show that the effect of resolution is modest, albeit sizable, at redshift $z = 0$ and more prominent at higher redshift, with differences in the enrichment history by a factor of ~ 2 . Similarly, Vogelsberger et al. (2018) find that the metallicity profiles of the IllustrisTNG simulated clusters vary by a factor of ~ 2 with resolution, as reported in Fig. 3. Indeed, increasing the resolution effectively enhances the star formation, especially at high redshift, as a consequence of the larger number of resolved small haloes that collapse first and in which gas cooling happens very efficiently. Since this effect is more prominent at high redshift, the pre-enrichment history in the simulations will change, resulting in a more efficient metal enrichment of the gas in the early epochs, that propagates till lower redshifts. As explicitly discussed by Martizzi et al. (2016) and Vogelsberger et al. (2018), numerical convergence is however rather slow and difficult to achieve. Furthermore, when numerical resolution is increased the sub-grid physical models in the simulation need to be re-calibrated to maintain the agreement with some reference observables, and this does not imply convergence of results in the enrichment properties.

Finally, the physical processes treated in the simulations, and their sub-grid implementation, also have a sizable impact on the final enrichment history

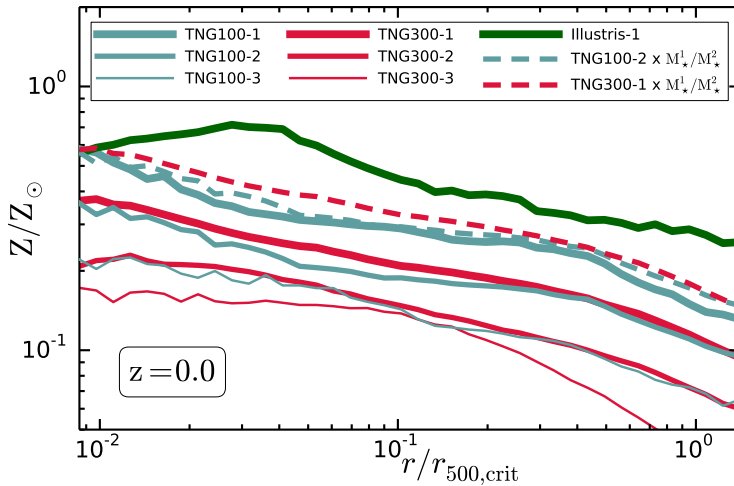


Fig. 3 Resolution effects on the median (total) metallicity profiles for simulated clusters extracted from the Illustris and IllustrisTNG simulations; taken from Vogelsberger et al. (2018). Different lines refer to different resolution runs, as in the legend. The total metallicity is expressed in units of the solar value.

and metal distribution in simulated clusters. In the following sections, we will outline the impact of the energy feedback scheme adopted on the distribution of metals in the ICM, in comparison to observations.

3 Abundance distribution in the ICM

A number of physical and dynamical processes can influence the distribution of metals in the ICM: galactic winds and AGN feedback, depletion of metal-rich gas due to cooling and consequent star formation or to dust formation, or dynamical processes like merging events, large-scale motions and ram-pressure stripping (see Schindler and Diaferio 2008, for a review). Therefore, the study of chemical abundances in the hot ICM provides invaluable information about the formation and assembly histories of the clusters as well as on the interplay between the galactic population and the surrounding diffuse medium. Also, the spatial distribution of specific heavy ions in the ICM, that are produced from different stellar sources on different time scales, carries the imprint of the star formation and assembly history of the cluster as well as the signatures of the feedback processes from stars and AGN. The comparison between the distribution of different elements and their abundance ratios can unveil precious information on the relative incidence of the stellar sources that released them.

In this section we review the main results on the ICM enrichment in cluster simulations with special attention to the spatial distribution of heavy elements, from the innermost regions out to the cluster boundaries.

Metallicity estimates in simulations

Similarly to many other thermodynamical quantities, also metal abundances can be computed in different ways from the intrinsic, three-dimensional properties characterizing the hot gas component in simulated clusters. This aspect is particularly important when comparing against observational datasets. In fact, measurements of chemical abundances in the ICM are typically derived from X-ray observations of the ICM spectral emission, which is essentially composed by a Bremsstrahlung continuum and emission lines of heavy ions (Werner et al. 2008; Böhringer and Werner 2010, Mernier et al., *subm.*, this issue). This measurement is therefore naturally sensitive to the emissivity of the gas.

In simulations, the value of metallicity for the gas contained in a given region is typically computed as

$$Z_w = \frac{\int w Z dV}{\int w dV} \rightarrow \frac{\sum_i Z_i w_i}{\sum_i w_i}, \quad (1)$$

where the second fraction is the discretized formula for the gas elements considered in the simulations. Specifically, Z_i and w_i are the metallicity and chosen weight of each gas element i selected. In general, two weighted averages are most commonly adopted, the *mass*-weighted value and the *emission*-weighted one. In the former the weight is simply the mass of the gas element, $w_i = m_i$. In the latter, the weight is the gas emissivity $w_i = m_i \rho_i \Lambda(T_i, Z_i)$, where m_i and ρ_i are the gas-element mass and density, and $\Lambda(T_i, Z_i)$ is the cooling function, which depends on the temperature (T_i) and global metallicity of the gas element. Depending on the definition adopted, the metallicity of the single gas element (Z_i) is given by the fraction between the metal mass and the gas or hydrogen mass associated to it. Similarly, in simulations where the single metal species are separately tracked, the weighted average expressed by eq. (1) can be calculated for individual metal abundances (Z_i^X , for the chemical element X).

For a more faithful comparison with X-ray data, one could generate synthetic X-ray observations out of the simulation outputs. To this scope, a number of groups have dedicated a significant effort, designing specifically suited X-ray simulators able to generate mock X-ray data mimicking the performances of existent and upcoming X-ray telescopes (Gardini et al. 2004; Heinz and Brüggén 2009; Biffi et al. 2012; ZuHone et al. 2014). Using this technique, Rasia et al. (2008) investigated possible observational biases in the X-ray derived metallicity measurements from simulated clusters by analysing mock *XMM-Newton* spectra. Their main findings are that iron abundances are well recovered with respect to the intrinsic simulation value whenever the gas plasma has a temperature higher than 3 keV or lower than 2 keV, while the multi-temperature structure of gas in the 2–3 keV temperature range typically leads to an overestimate in the spectroscopic measurement. Oxygen, on the contrary, is overall well measured for low-temperature ($T < 3$ keV) systems while it can be overestimated for hotter clusters. We note that the test presented in Rasia et al. (2008) was specifically done for CCDs and that oxygen, in particular, is measured at the limits of the energy band sensitivity. A similar

approach has been adopted by Cucchetti et al. (2018), to predict the capabilities of the X-ray Integral Field Unit (X-IFU) on board the next-generation European X-ray observatory *Athena* in reconstructing the chemical properties of the ICM from mock observations of a sample of simulated galaxy clusters. In this work the authors show that emission-measure-weighted metallicity values (obtained from (1) with $w_i = m_i \rho_i$) computed from the simulations can be accurately recovered from the spectral analysis of the mock X-ray images up to redshift $z \approx 2$.

3.1 Global distribution

From the global distribution of particular elements in the ICM valuable information can be inferred on the underlying distribution of different types of supernovae or on the feedback processes in the ICM.

The influence of varying the IMF and therefore the relative number of SNIa and SNII is in fact visible from the metallicity distributions shown in Tornatore et al. (2007). Typically, they find that SNII enrichment (e.g., oxygen) dominates patchy high-density regions located in the vicinity of star-formation sites, while AGB and SNIa contribute more to the diffuse enrichment. The contribution of SNII is more evident when a top-heavier IMF is assumed, which enhances the relative number of massive SNII-progenitor stars (see also Fabjan et al. 2008). These simulations accounted only for stellar feedback, but changing the details of this feedback scheme included also has an impact on the global distribution. In particular, Tornatore et al. (2007) show that increasing the winds strength has the general effect of increasing the diffusion of metals. This effect is more significant for oxygen than for iron, because winds are up-loaded with star-forming gas particles and therefore mostly enriched by SNII.

From Fig. 4 we can see how the global distribution of oxygen (mass-weighted) abundance in the ICM changes depending on the feedback scheme included in the simulations. The two clusters reported (see Rasia et al. 2015, for more details on the simulations) are the same object, simulated with different feedback schemes: on the left, stellar and AGN feedback are both included (‘AGN’ simulation run), while on the right only the former is considered (‘CSF’ simulation run). Visibly, the present-epoch level of oxygen enrichment and its spatial distribution are very different. In the ‘AGN’ case the gradient with cluster-centric distance is flatter and more homogeneous especially at large radii with respect to the ‘CSF’ map, where the distribution is clumpier, more centrally-peaked and with more peaked sub-structures (e.g. the one in the right-most periphery) (see also Fabjan et al. 2010). Given that oxygen is released by SNII on short time scales and therefore traces recent star formation, the more homogeneous distribution in the ‘AGN’ cluster is an evidence of pre-enrichment. Indeed, AGN feedback at early epochs is able to widely distribute metal-enriched gas outside small haloes already before the star formation peak (see Biffi et al. 2017, 2018). This effect is ultimately reflected in

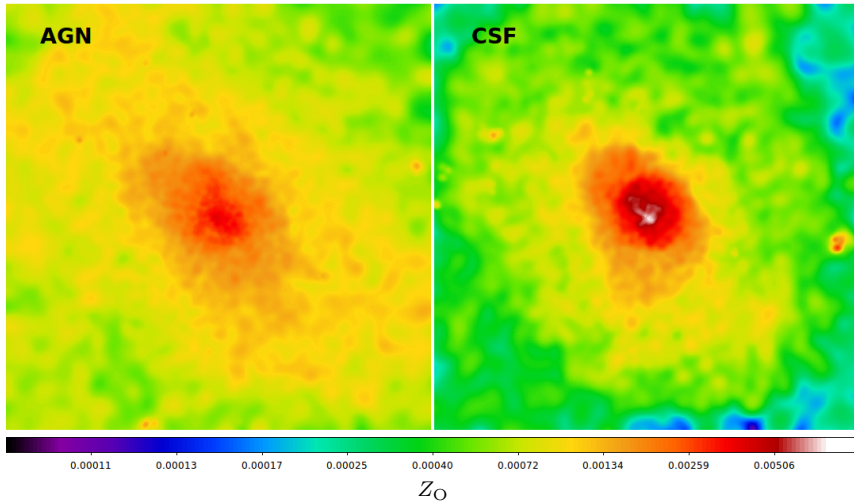


Fig. 4 Mass-weighted oxygen abundance maps for a cluster at $z = 0$, simulated with stellar and AGN feedback (‘AGN’; left) and only with stellar feedback (‘CSF’; right). The oxygen abundance, Z_{O} , is the mass fraction w.r.t. to hydrogen. Each map has a side of 2 Mpc, is projected for 2 Mpc along the line of sight, and is centered on the minimum of the cluster potential well. The cluster belongs to the simulation set for which results on the ICM metal enrichment have been presented in Biffi et al. (2017, 2018).

the present-day radial profiles of clusters, especially in the outermost regions (see further discussion in Sec. 3.4).

3.2 Radial metallicity profiles

As inferred from the maps in Fig. 4, the study of the metallicity profiles in clusters and of their gradient provides direct information on the efficiency of the feedback history of galaxy clusters.

Observationally, radial metallicity profiles of the ICM have been extensively investigated since the first explorations of bright nearby clusters with *ASCA* and *Beppo-SAX*. The most recent X-ray observatories, namely *Chandra*, *XMM-Newton* and *Suzaku*, were able to map the ICM enrichment from the innermost region out to the cluster boundaries (see Mernier et al., *subm.*, this issue). Already from the first observational evidences, it has been clear that ICM metallicity profiles present gradients with differences in the central slope depending on the cool-core-ness of the cluster.

In cosmological hydrodynamical simulations of galaxy clusters radial distribution of the total ICM metallicity or of specific element abundances (when individually traced) have been investigated at various levels of complexity, in terms of the physical processes treated within the code. Many numerical works that include only stellar feedback typically found iron abundance profiles steeper than the observed profiles. For instance, Valdarnini (2003) analysed a

set of simulations of regular galaxy clusters characterized by a quiet dynamical state, following the production of iron from SNIa and SNII, and found that the simulated iron profiles showed a radial decrease in the outer regions that was clearly steeper than the observational profiles by De Grandi and Molendi (2001). This steeper gradients of the metallicity profiles have been connected to a lack of an efficient feedback, such as the one associated to AGN (Sijacki and Springel 2006; Fabjan et al. 2010; Planelles et al. 2014; Biffi et al. 2017).¹

Tornatore et al. (2007), despite including only stellar feedback, found a better agreement with observed profiles by Vikhlinin et al. (2005), but showed how the details of the feedback model (e.g. the velocity of the winds) affect the final shape of the iron abundance profile. As remarked by the authors, not only the ICM metallicity profiles but also the properties of the galaxy population must be successfully reproduced. However, simulations based on stellar feedback only typically produce central cluster galaxies that are bluer and more star forming than observed. A recent investigation by Martizzi et al. (2016), including both stellar and AGN feedback, also showed metallicity gradients in clusters simulated with an AMR code that are fairly consistent with the observational data by Leccardi and Molendi (2008) and Matsushita et al. (2013b), despite a disagreement in the normalization. A flatter shape towards the outskirts is also recovered, when the emission-weighted metallicities are computed. A better agreement with recent observed profiles, also in term of normalization, was instead shown for the ICM iron profiles in simulated galaxy clusters by Biffi et al. (2017, 2018) and Vogelsberger et al. (2018), with different numerical codes, resolution and implementation of the main feedback processes. We will discuss more later in Section 3.4 how the effect of early AGN feedback in numerical simulations of clusters helped reproducing the flat outskirts profiles found by X-ray observations.

Other than iron or total metallicity, the distribution of other elements such as oxygen or silicon, and their relative abundance with respect to iron, provide valuable information on the distribution of SNIa and SNII. Despite previous findings indicating an excess of Fe with respect to SNII products in the center, many recent observations suggest that abundance ratios are found to be remarkably uniform from the core out to large cluster-centric distances (e.g. Sato et al. 2008; Sakuma et al. 2011; Matsushita et al. 2013a; Simionescu et al. 2015; Mernier et al. 2017, Mernier et al., *subm.*, this issue). From the simulation side, recent results by Biffi et al. (2017) show similarly flat abundance ratio profiles compared to X-ray data for the Coma, Centaurus and AWM7 galaxy clusters (Sato et al. 2008; Sakuma et al. 2011; Matsushita et al. 2013a), with a mild increasing trend towards the center (see also Planelles et al. 2014). These results are reported in Fig. 5, for the Si/Fe (upper panel) and O/Fe (lower panel) abundance ratios. The median abundance ratio profiles from the simulated clusters by Biffi et al. (2017) are compared with the X-ray data for the Coma, Centaurus and AWM7 clusters and with the mean profiles reported

¹ The different slope of the metallicity profiles in simulations with and without AGN feedback can be seen from the comparison in Fig. 8.

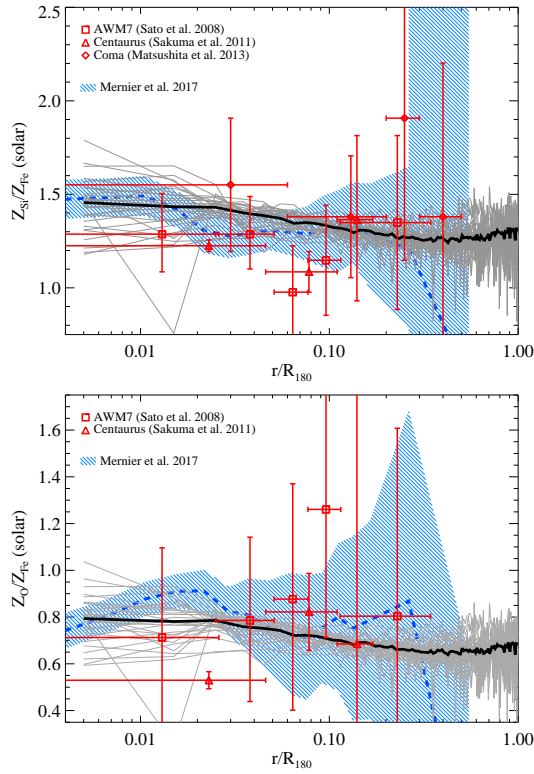


Fig. 5 Median abundance ratio profiles as a function of cluster-centric distance for the set of simulated clusters presented in Biffi et al. (2017) (black solid line; individual profiles are marked as gray thin lines). *Upper panel*: Si/Fe; *lower panel*: O/Fe. For comparison, observational data by Mernier et al. (2017) (blue shaded areas and dashed lines), Sato et al. (2008) (red squares), Sakuma et al. (2011) (red triangles) and Matsushita et al. (2013a) (red diamonds) are reported as well; all abundances are rescaled with respect to the reference solar values by Anders and Grevesse (1989).

by Mernier et al. (2017) for a sample of 44 nearby cool-core galaxy clusters, groups, and ellipticals (from the CHEERS sample; Mernier et al. 2016; de Plaa et al. 2017). From the comparison between simulated and observed profiles, we note a remarkable agreement in the intermediate/outer radial range for both abundance ratios, especially considering the scatter around the median profiles. Interestingly, this result holds not only for the trend but also for the normalization, despite the possible uncertainties due to the set of stellar yields adopted in the model. In the Si/Fe case, in particular, the median simulated profile is in very good agreement with observational data also in the central region. Instead, a mild discrepancy is observed at small radii, $r \lesssim 0.04 R_{180}$, between the median simulated O/Fe profile and the one by Mernier et al. (2017), although simulated and observed data are still consistent within the scatter. We remind nevertheless that the accurate measurement of oxygen abundances with CCD instruments is still very challenging.

In this respect, also the Si/Fe and O/Fe profiles presented by Vogelsberger et al. (2018) are consistent with the observational values reported in Fig. 5, given the large error bars in the observed profiles (see Fig. 7 — r.h.s. panels — in Vogelsberger et al. 2018). Nevertheless, the abundance ratios by Vogelsberger et al. (2018) present an opposite tendency to slightly increase from the center towards the outskirts with respect to the flatter profiles by Mernier et al. (2017).

In both these simulation sets the relative contribution from SNIa and SNII to the ICM metal content as a function of radius has been inspected directly, confirming that the bulk of the metal production (in terms of mass fraction) at all radii is largely dominated by SNII. Also, in both cases abundance ratio profiles, such as Si/Fe and O/Fe, are very good tracers of the SN relative contributions and of the different ICM enrichment histories, mirroring in fact in the different trends with radius highlighted above.

3.3 Cluster core

Observations of strongly peaked X-ray emissivity in the centre of relaxed clusters suggest the presence of significant cooling flows in the central regions of galaxy clusters as a consequence of the radiative losses of the ICM in the core (Fabian 1994), that would become denser and colder initiating a runaway cooling process. Even though observations show no presence of such massive cooling flows, suggesting that a central source of heating (e.g. AGN feedback) must be at play, the low-entropy dense gas does sink towards the core of the so-called cool-core (CC) clusters (named as such by Molendi and Pizzolato 2001). Differently, non-cool-core (NCC) clusters are typically observed to have nearly isentropic gas cores at a higher entropy level (e.g. Maughan et al. 2008). A definite distinction from CC, nonetheless, is still largely debated and the definition of CC itself based on the central thermal properties (e.g. central density or temperature drop, central cooling time or mass deposition rate) can vary substantially from author to author (Barnes et al. 2018; Hudson et al. 2010, and references therein). Starting with *Beppo-SAX* and *XMM-Newton* observations of large cluster samples in the early 2000s (e.g., De Grandi and Molendi 2001; De Grandi et al. 2004; Leccardi and Molendi 2008), X-ray observations indicated that also the central gradient of the ICM metallicity is different depending on the cluster cool-core-ness (see also Mernier et al., *subm.*, this issue).

From the theoretical point of view, cosmological hydrodynamical simulations have struggled for many years to reproduce the observed diversity between CC and NCC clusters: simulated clusters were typically characterised by higher central metallicities than observed, independently of the central entropy level, that was generally high like in NCC systems (Dubois et al. 2011). Only recently, cosmological hydrodynamical simulations have been able to recover the observed diversity of CC and NCC populations (Rasia et al. 2015; Hahn et al. 2015; Barnes et al. 2018), both in thermal and chemical properties. In

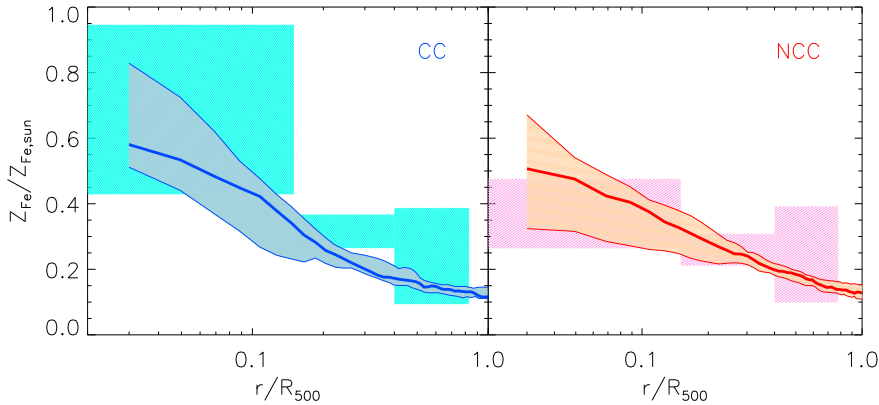


Fig. 6 CC (left) and NCC (right) median metallicity profiles for the simulated clusters at $z = 0$ presented in Rasia et al. (2015) (solid lines, with 16th and 84th percentiles around the median). Shaded boxy areas in the two panels represent observational data for local ($z < 0.2$) clusters by Ettori et al. (2015). All abundances are rescaled with respect to the reference solar values by Anders and Grevesse (1989).

agreement with observations, these numerical investigations have found that the metallicity profiles are flatter for NCC systems, whereas they present a peak in the core of CC clusters, for which the metallicity gradients result to be steeper (see also Martizzi et al. 2016; Vogelsberger et al. 2018). This is shown in Fig. 6, where we report the median CC and NCC Fe profiles (l.h.s. and r.h.s. panel, respectively) for the sample of simulated clusters presented in Rasia et al. (2015) and Biffi et al. (2017), compared to observations by Ettori et al. (2015).

As shown in Fig. 6, while CC present a metallicity peak towards the centre ($r < 0.15 R_{500}$), NCC show instead a lower central enrichment level. This chemical diversity anti-correlates therefore with the entropy level: CC are characterised by a decreasing entropy profile towards the center, with a core entropy lower than NCC systems, where, as previously said, the entropy profiles flattens to higher values.

This anti-correlation between entropy and metallicity in the cores of galaxy clusters is for example shown in *XMM-Newton* observations by Leccardi et al. (2010). In Fig. 7, the relation between core entropy and central Fe abundance is reported for the sample of simulated clusters analysed in Biffi et al. (2017) and compared to the observational data by Leccardi et al. (2010). Similarly to observations, the central entropy gradient can be quantified by the pseudo-entropy ratio $\sigma = (T_{\text{sl,IN}}/T_{\text{sl,OUT}}) * (EM_{\text{IN}}/EM_{\text{OUT}})^{-1/3}$, with the spectroscopic-like temperature (T_{sl} ; Mazzotta et al. 2004) and emission measure (EM) computed within the projected “IN” ($r < 0.05 R_{180}$) and “OUT” ($0.05 R_{180} < r < 0.2 R_{180}$) regions (e.g. Leccardi et al. 2010; Rossetti et al. 2011). The Fe abundance is also computed within the IN region used to calculate σ . The comparison shows that the two quantities anti-correlate with a similar slope to observed one, with CC clusters that are more metal-rich in the

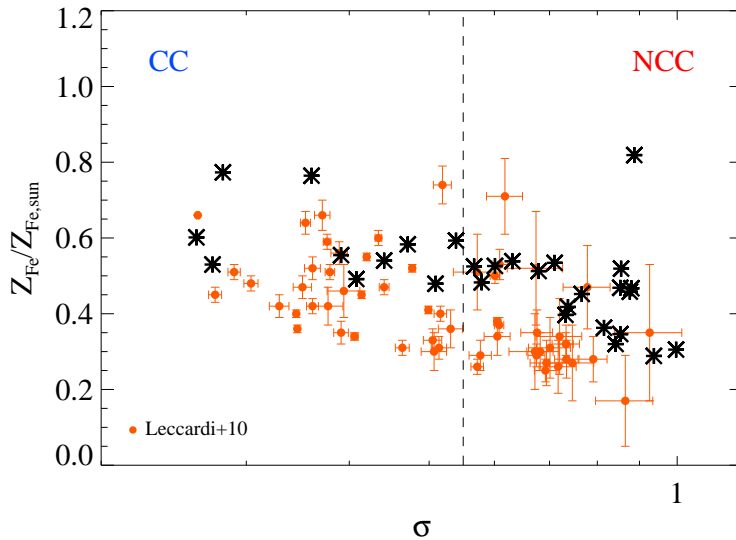


Fig. 7 Relation between central metallicity and entropy for the simulated clusters from the sample presented in Biffi et al. (2017) (black asterisks), compared to data by Leccardi et al. (2010) (orange circles with error bars). All abundances are rescaled with respect to the reference solar values by Anders and Grevesse (1989).

center with respect to NCC clusters. Essentially, this result indicates that the low-entropy gas is also metal rich. For the dense low-entropy gas the radiative cooling is in fact very efficient and star formation can take place, consequently enriching the gas with metals. Given that diffusion of metals takes place on long time-scales, the metals trace therefore the gas region where they have been injected and can be diluted only if the ICM itself under-goes mixing processes. Thus, since the low-entropy gas is also the one preferentially sinking towards the center of the clusters, a low-entropy high-metallicity core can form. In NCC systems, on the other hand, the low-entropy metal-rich gas is likely to be more diffuse rather than concentrated in the innermost region. A likely explanation for this is related to the effect of merging events that displace and distribute the metal-rich low-entropy gas.

In Biffi et al. (2017) the authors also show the central entropy-metallicity relation for clusters simulated without the inclusion of AGN feedback, finding that the majority of systems has high core entropy (like NCC) but also a central metallicity that is far larger than observed, making the entropy-metallicity relation too steep compared to data.

More generally, however, we note that differences between various simulation results still persist in the modelling of cluster cores, given that the detailed metal distribution in those regions is highly sensitive to the details of the galaxy formation model, especially the specific AGN feedback implementation.

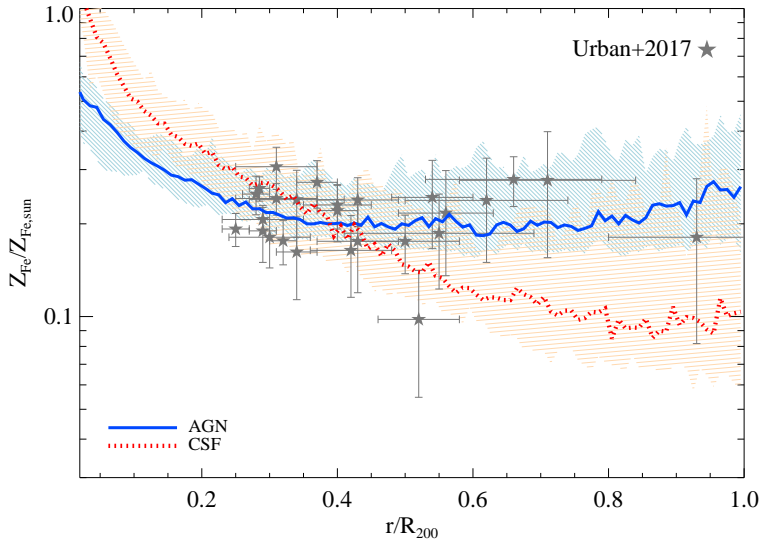


Fig. 8 Comparison between Fe median profiles in the same simulations including only stellar feedback (‘CSF’) or both stellar and AGN feedback (‘AGN’). The scatter on the profiles is marked by the shaded areas. For comparison, we also report data by Urban et al. (2017) for the outskirts ($r > 0.2 R_{200}$) of local galaxy clusters (symbols). All abundances are rescaled with respect to the reference solar values by Anders and Grevesse (1989).

3.4 Cluster outskirts

The simulation results on cluster metallicity profiles (e.g. shown in Fig. 6) are in line with X-ray observations not only in the central regions but also in the outskirts, where little variance is found between CC and NCC profiles. In particular, X-ray observations indicate a remarkably uniform ICM enrichment beyond the cluster core, out to R_{500} or more (Fujita et al. 2008; Leccardi and Molendi 2008; Werner et al. 2013; Simionescu et al. 2015; Urban et al. 2017).

At intermediate and large cluster-centric distances the metallicity and abundance ratio profiles are all found to be relatively flat (see Mernier et al., *subm.*, this issue), in both CC and NCC clusters (e.g. Ettori et al. 2015, as shown in Fig. 6).

The shape of the abundance profiles, instead of their amplitude, is a key information to constrain the impact that different feedback mechanisms have on the ICM enrichment pattern, since degeneracies among the assumptions of the chemical model can play a role in the normalization of the profiles (e.g. Romeo et al. 2006; Tornatore et al. 2007; Fabjan et al. 2008). Early results from cosmological hydrodynamical simulations typically found steeper profiles than observed, with a clear decreasing trend with increasing radius. Later on, many groups started to include more efficient energy feedback processes, such as feedback from AGN, to alleviate the central overcooling in groups and clusters (e.g. Borgani and Kravtsov 2011, and references therein), which eventually

allowed to successfully reproduce many realistic properties of galaxy clusters. Despite the persisting challenges to reproduce correctly the core properties, the role played by AGN feedback was found to be effective in producing flatter ICM metallicity profiles at large radii $\gtrsim 0.2-0.3 R_{vir}$ (Sijacki and Springel 2006; Fabjan et al. 2010).

This can be seen from the profiles reported in Fig. 8, based on simulation results presented in Biffi et al. (2017, 2018). In the figure, we show the median emission-weighted projected iron abundance profiles (with respect to solar reference values by Anders and Grevesse 1989) for a sample of 29 simulated clusters. The simulations include self-consistent treatments for gas cooling and star formation, metal enrichment from stellar evolution, and energy feedback from both stellar and AGN sources (‘AGN’ run; blue curve and shaded area). For comparison, we also show the median profile for the same set of clusters simulated without AGN feedback (‘CSF’ run; red curve and shaded area). By inspecting the shape of the two profiles, it is visible that the inclusion of AGN feedback in the simulations produces an overall flatter profile than the ‘CSF’ run, especially in the outskirts ($r \gtrsim 0.2 R_{200}$) where the former is in better agreement with recent X-ray data from Urban et al. (2017). Despite the scatter among different clusters present at large radial distances, the difference between the two runs is well defined: while the ‘CSF’ profile significantly declines, the ‘AGN’ profiles remains flat, indicating a uniform enrichment in the outer regions.

The origin of this uniformity cannot be ascribed to the ongoing activity of the central AGN because not even an efficient AGN feedback can be able to displace significant amount of metal-enriched gas from the central regions out to the virial radius at low redshifts, especially in massive clusters where the potential well is very deep. Thus, the uniform enrichment in the outskirts of present-day massive galaxy clusters must be the result of a pre-enrichment in which the role of early feedback processes appear to be crucial. Recent observational results and their quantitative agreement with those from cosmological hydrodynamical simulations further support this picture.

Detailed investigations of the IllustrisTNG simulations by Vogelsberger et al. (2018) on the origin of metal-enriched gas within clusters at $z \sim 0$ show that the majority of it was accreted from the proto-cluster region. In particular, Vogelsberger et al. (2018) show that the average metallicity of the gas residing in the 5 Mpc-radius around the cluster progenitors is already high at $z \sim 2$ (see also Biffi et al. 2017) and close to the typical metallicity of the outer profiles, so that its later accretion onto the cluster does not alter the typical outskirts enrichment and the outer profiles remain nearly constant and flat down to $z \sim 0$. The metallicity of the accreted gas is also quite universal across their large cluster sample. Similar results were found by Biffi et al. (2018), who investigated the origin of the metal-rich gas found in the outskirts (roughly $R_{500} < r < R_{200}$) of a study sample of four simulated clusters, selected to have different masses and core properties. By directly tracking back in time and space the hot gas particles residing in the outskirts at $z = 0$ the authors showed that at higher redshift they were residing in the proto-cluster region,

mainly outside the progenitor, and are later accreted onto the forming cluster. At $z \sim 2$, the tracked gas comprises both pristine particles and highly-enriched ones, which makes the average metallicity of this accreted material already very similar to that in the outskirts. In this study, the authors also show that the relative contribution from SNIa and SNII to the enrichment of this tracked gas does not depend on the environment where it resides up to $z \sim 2$.

These results further indicate that the bulk of the outskirts ICM was enriched earlier inside galaxies in the proto-cluster region and then displaced on larger scales by early AGN feedback. At $z \gtrsim 2$, in fact, the potential well of galaxies is shallower and AGN feedback can be more effective in removing pre-enriched gas beyond the galaxy boundaries (see also McCarthy et al. 2011) and far from active star-formation sites, contributing to the diffuse enrichment of the inter-galactic medium. As shown by simulations, AGN feedback has a key role since stellar feedback alone is not as effective in distributing the enriched material far from the star formation sites, where it is efficiently locked back into newly formed stars (Biffi et al. 2018).

4 Evolution of the ICM metallicity

The study of the ICM metallicity at different cosmic times is crucial to confirm the pre-enrichment scenario as well as to assess the enrichment history of galaxy clusters.

From the observational side, how much the ICM metallicity evolves with time is still a matter of debate, although recent X-ray observational studies suggest a mild evolution in the central regions (especially for CC systems) and a nearly constant enrichment level at large cluster-centric distances (Ettori et al. 2015; McDonald et al. 2016; Mantz et al. 2017, and Mernier et al., *subm.*, this issue).

The ICM pre-enrichment picture, advocated to explain the flat radial profiles in present-day cluster outskirts found by both X-ray observations and simulations, is also consistent with the very mild redshift evolution of the ICM metallicity below $z \sim 2$.

Recent studies based on state-of-the-art simulations accounting a large variety of physical processes, including AGN feedback, have shown that the average ICM metallicity and iron-abundance within R_{500} is nearly invariant between $z \sim 1.5$ – 2 and $z = 0$ (Biffi et al. 2017; Vogelsberger et al. 2018). This is consistent with the flat metallicity profiles at large radii, throughout that redshift range (e.g. Martizzi et al. 2016). These recent different simulations all showed that the metallicity profiles present a mild tendency to become flatter with time, although changes in the normalization are typically smaller than $\lesssim 10$ – 20% between $z = 2$ and $z = 0$.

Concerning the central regions in clusters, an early study based on simulations without AGN feedback by Fabjan et al. (2008) showed a significant increase of metallicity in cluster central regions ($r < 0.2 R_{180}$) below redshift $z \sim 1$, with the specific degree of evolution depending on the assumed IMF. As

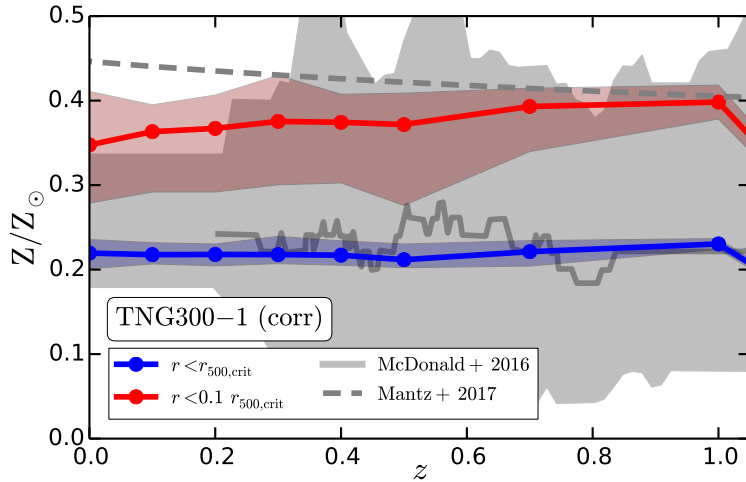


Fig. 9 Median redshift evolution of mass-weighted average metallicities for clusters in the IllustrisTNG suite; taken from Vogelsberger et al. (2018). Data for two radial ranges are reported, inner ($r < 0.1 R_{500}$) and total within R_{500} , and compared against observations by McDonald et al. (2016) and Mantz et al. (2017).

discussed by those authors, this positive evolution can actually be the spurious product of the excess of star formation in the central cluster regions, due to the lack of an efficient feedback process (only stellar feedback was included in those simulations). In fact, more recent simulations including also the treatment of AGN feedback, find an overall weak evolution of the ICM metallicity with time also in the cluster core. This is for instance shown by Vogelsberger et al. (2018), as reported in Fig. 9, for a large set of simulated clusters from the recent IllustrisTNG simulation suite, including both CC and NCC systems. Below $z \sim 1$ simulation data are consistent with no evolution, both in the core ($r < 0.1 R_{500}$) and within the global R_{500} region (respectively, red and blue curves and shaded areas). From Fig. 9, we note that the scatter on the median evolution of the metallicity averages is significantly small for the global R_{500} region: this stresses the universality of the result among different clusters and is a further evidence of pre-enrichment, since the global mass-weighted value is heavily biased towards the enrichment level of the outer regions, where most of the mass is located. Similar results, were also shown by Biffi et al. (2017) up to $z \sim 2$. In the cluster core, $r \lesssim 0.1 R_{500}$, the scatter is instead larger, due to the more important role played in those regions by astrophysical processes such as cooling, star formation and feedback, but still it is significantly smaller than observed (e.g. compared to McDonald et al. 2016; Mantz et al. 2017). A stronger evolution of the core enrichment level, like that reported by other X-ray works (Ettori et al. 2015), could be ascribed mainly to the evolution of the CC population, since X-ray-selected samples are biased towards those.

5 Metal budget in clusters and groups

Differently from what previously suggested from X-ray observations, the universality of the ICM enrichment seems to concern not only the time evolution but also the various cluster scales, ranging from groups to clusters, as indicated by theoretical and numerical studies. In the past, X-ray observations of small-mass systems like giant elliptical galaxies and groups of galaxies typically indicated a lower enrichment level of the hot gas component with respect to massive galaxy clusters (Fukazawa et al. 1998; Baumgartner et al. 2005; Rasmussen and Ponman 2007, 2009; Sun 2012; Mernier et al. 2016; Yates et al. 2017, see also Mernier et al., *subm.*, this issue, for more details), especially in their cores (10–15% of R_{500}). Only recently, these measurements for the core region have been revised upwards (see results from the CHEERS sample, Mernier et al. 2018, and Truong et al. 2018), confirming an essentially negligible dependence of the metallicity on the system temperature.

From the theoretical side, different studies, based both on simulations (Davé et al. 2008; Fabjan et al. 2010; Planelles et al. 2014; Liang et al. 2016; Barnes et al. 2017; Dolag et al. 2017; Truong et al. 2018) and on semi-analytical models (Yates et al. 2017, for a recent study), have shown that the level of enrichment from groups to rich clusters is essentially similar. In fact, only a very weak dependence of the metallicity on the system mass is found, with the intragroup gas slightly more enriched than the ICM in massive clusters. This has been shown in a recent study by Barnes et al. (2017), where the authors investigate the relation between iron abundance and system temperature, for the C-EAGLE sample of 30 simulated clusters with masses in the range $7 \times 10^{13} \lesssim M_{500}[M_{\odot}] \lesssim 1.2 \times 10^{15}$. In Fig. 10 they compare these results with those from other two sets of EAGLE simulations including clusters and smaller groups (grey circles and purple diamonds in the figure), and with consolidated observational data recompiled by Yates et al. (2017). The simulated relation shows good agreement with observations especially in the range $T_{500,spec}^X \gtrsim 1$ keV, whereas the observed iron abundance in low-temperature groups is found to be lower than in simulations, which produce a relatively flat mass-weighted metallicity-spectroscopic temperature relation.

Also Truong et al. (2018) found a relatively shallow relation between metallicity and temperature, from group to cluster scales, both in the central regions (within 10% of R_{500}) and in the global R_{500} region. For this study, the authors investigate a large sample of simulated clusters obtained with an improved, state-of-the-art version of the SPH code GADGET-3, including the sample of massive clusters for which the chemical content and enrichment history has been shown to agree with a variety of observational data in Biffi et al. (2017, 2018). Simulation results are in good agreement with recent data by Mantz et al. (2017) and from the CHEERS sample (de Plaa et al. 2017, including the updated metallicity measurements presented by Mernier et al. 2018). Truong et al. (2018) show that the dependence of gas metallicity on the system scale is very shallow, basically consistent with being flat, also when the true mass, instead of temperature, is considered. Furthermore, they show that the evolu-

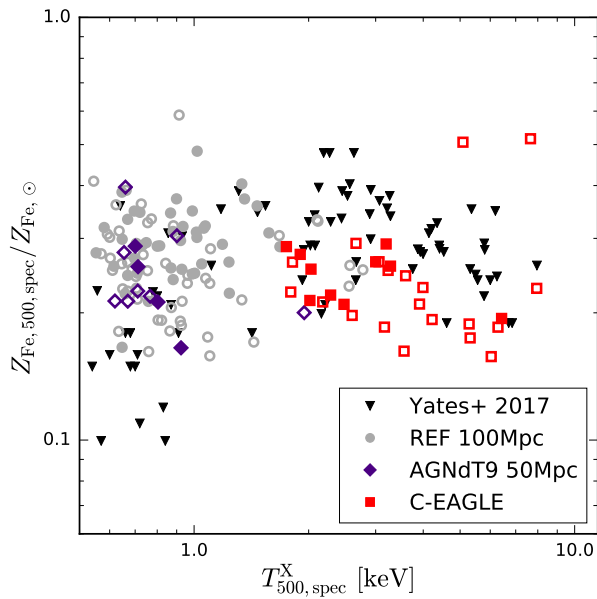


Fig. 10 Mass-weighted iron abundance measured within the spectroscopic radius $R_{500,spec}$ as a function of the spectroscopic temperature, at $z = 0.1$, for the C-EAGLE clusters; taken from Barnes et al. (2017). The homogenized observational data reported by Yates et al. (2017) are also reported for comparison.

tion of this relation with time is negligible between $z \sim 1.5$ and $z = 0$. Despite an average enrichment level similar to clusters, simulations show that there is a large scatter in metallicities in low-temperature (low-mass) systems (Davé et al. 2008; Fabjan et al. 2010; Planelles et al. 2014; Liang et al. 2016; Truong et al. 2018; see also Barnes et al. 2017, reported in Fig. 10). This is related to the diversity of the impact that gas-dynamical processes and AGN feedback have on the enrichment pattern in smaller systems, given their shallower potential wells.

In a similar set of simulations from the Magneticum Pathfinder Project, Dolag et al. (2017) investigate the metallicity-temperature relation in a large sample of simulated massive clusters ($T > 2$ keV), considering various chemical species separately. These results are reported in Fig. 11. Dolag et al. (2017) find essentially flat metallicity-temperature simulated relations not only for iron (top panel in Fig. 11) but also for all the other elements considered, with typical values in agreement with observational data in most of the cases (we show, for instance, the case of Si/Fe and Si/Fe in the bottom panel of Fig. 11). Compared to observations by de Plaa et al. (2007), Dolag et al. (2017) find differences in the normalization of the simulated metallicity-temperature relation only for a few elements among those followed in the simulations, namely for Ne, Ca and Ni, which can nevertheless be related to the set of yields adopted.

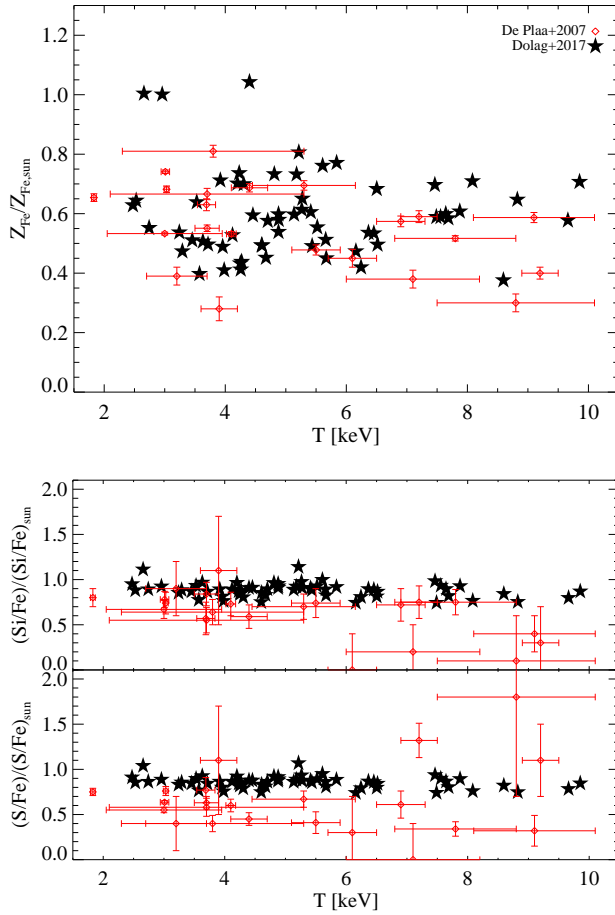


Fig. 11 ICM Fe metallicity (top) and abundance ratios (Si/Fe and S/Fe; upper and lower insets in the bottom panel, respectively) for observed clusters by de Plaa et al. (2007) (red diamonds with error bars) and simulated clusters by Dolag et al. (2017) (black stars), as a function of the system temperature. All abundances are measured within R_{2500} , and the temperature is the mean value within R_{500} .

6 Current limitations and final remarks

The study of the ICM chemical enrichment through the cosmic time provides invaluable information on the evolution of cosmic baryons, the past star-formation history of clusters and the gas-dynamical interaction between galaxies and surrounding gas in the overdense cluster environment. In this review article, we revised and discussed the most important results obtained in this field from a theoretical perspective, with a special focus on numerical simulations.

In particular, the modelling of the chemical properties of the ICM in state-of-the-art cosmological hydrodynamical simulations has made huge steps for-

ward in the last years. The description of the main processes driving the baryonic physics of the hot plasma in groups and clusters has now reached an unprecedented level of complexity, and simulations succeed in reproducing a large variety of observational features. The emerging global picture indicates that an early enrichment of the gas in the proto-cluster region must take place in order to explain the observed (i) uniformity of the enrichment level over large spatial scales in the outer regions of local clusters and across different mass scales, from groups to massive systems, and (ii) the time invariance of the chemical enrichment below redshift $z \sim 1-2$.

Despite their successes, cosmological simulations still need to be improved in order to consistently reproduce observed chemical and thermodynamical properties of both clusters and galaxies, accounting for the various physical processes in place. The chemical enrichment of cosmic baryons and its evolution are in fact sensitive to several factors, other than the details of the chemical evolution modelling itself. Complex physical and dynamical processes in clusters contribute to mix and distribute metals over large spatial scales, and to shape the final ICM enrichment level (see Schindler and Diaferio 2008, for a review). Among these, we recall stellar feedback in the form of galactic winds, ram-pressure stripping, dynamical mixing due to large-scale gas motions, buoyancy of gas bubbles associated to AGN jets, metal diffusion, and depletion of heavy ions due to dust formation (Churazov et al. 2001; Montier and Giard 2004; Rebusco et al. 2005, 2006; Simionescu et al. 2008, 2009; Kirkpatrick and McNamara 2015). The treatment of these phenomena into the simulations, and their specific implementation, can therefore impact in a non-trivial way the chemical properties of the ICM. This was discussed in the previous sections, in particular, about the various feedback processes accounted for in simulations.

The treatment of dust, for instance, should be certainly included in future simulations of cosmic structures and galaxy clusters, as it is an important component involved in the gas cooling and metal depletion. So far, the effects of dust have been poorly investigated in cosmological chemo- hydro-dynamical simulations of galaxy clusters (see preliminary works by Aguirre et al. 2001; Pointecouteau et al. 2009; da Silva et al. 2009), being mainly explored via post-processing computations coupled with numerical simulations of galaxies and clusters (e.g. Granato et al. 2015). Recently, a first implementation of the processes affecting the formation and evolution of dust (in the form of carbonaceous and silicate dust grains) in SPH simulations has been presented by Gjergo et al. (2018). In this work, differences are found with respect to the observed amount of dust in low-redshift galaxy clusters, although the trend of dust abundances over metallicity in local galaxies is reasonably reproduced. Further detailed investigations in this direction are therefore strongly required, for instance to estimate the contribution of dust to the formation of molecular gas, a primary ingredient for more refined models of star formation. Moreover, a self-consistent implementation of dust formation and evolution in cluster simulations is crucial to compute more precisely observational properties of simulated objects by means of radiative transfer post-processing. This is essential for multi-wavelength studies of simulated clusters and of their member

galaxies, that can be compared with a vast range optical and infrared observations. A successful simulation, in fact, should correctly reproduce both the large-scale cluster properties and the galactic population as well.

In this respect, a limitation of many current simulations of large cosmological volumes is still represented by resolution. Increasing the numerical resolution is a necessary step to consistently resolve galaxies (i.e. the central Brightest Cluster Galaxy as well as satellites) within clusters. In fact, the study of the processes that determine the chemical properties of galaxy clusters are strictly linked to the star formation and metal production histories of cluster galaxies. The quest for higher resolution is therefore a *conditio sine qua non* to study the complex interplay between galaxies and surrounding medium, via energetic and chemical feedback. These processes need to be captured in great detail especially at high redshift, when galaxies in the proto-cluster region are likely to enrich and eject gas out to large distances (see e.g. the recent study by Gupta et al. 2018).

Given the impact of the adopted yields and related parameters (e.g. mass limits for the different stellar phases) on the resulting ICM enrichment, it is crucial that numerical and observational improvements are accompanied by refined calculations of these pillar of stellar evolution models. In fact, the large uncertainties that are still present in these quantities directly affect the normalization of the predicted profiles and global enrichment levels, leaving the accurate comparison between simulations and observations, in terms of absolute values, still unsettled.

As demonstrated by the successful results obtained in the recent years, simulations and observations of the ICM chemical enrichment must definitely be combined in order to interpret the vast amount of data that up-coming X-ray telescopes will provide and to improve our theoretical understanding of the ICM chemo- and thermo-dynamics. In this respect, we remind that so far ICM chemical abundances of simulated clusters, both in terms of metal distribution and evolution, have always been compared against observational data obtained with CCD cameras on board past and current X-ray telescopes. Nevertheless, the advent of high-spectral-resolution micro calorimeters on board next-generation X-ray missions, such as *Athena* and *XRISM*, will likely open a new scenario with new challenges and further possible explorations, as it was demonstrated by *Hitomi* observations of the Perseus cluster (Hitomi Collaboration et al. 2018; see also the discussion in Mernier et al., *subm.*, this issue).

Acknowledgements V.B. is thankful to Elena Rasia and Stefano Borgani for useful suggestions that helped improving the manuscript, and to Klaus Dolag for kindly providing the simulation data reported in Fig. 10. She wishes also to thank Umberto Maio and partial funding support from a grant of the German Research Foundation (DFG), number 390015701. F.M. is supported by the Lendület LP2016-11 grant awarded by the Hungarian Academy of Sciences. SRON is supported financially by NWO, the Netherlands Organization for Scientific Research. P.M. acknowledges support from Russian Science Foundation (grant 14-22-00271).

References

- A. Aguirre, L. Hernquist, J. Schaye, N. Katz, D.H. Weinberg, J. Gardner, Metal Enrichment of the Intergalactic Medium in Cosmological Simulations. *ApJ* **561**, 521–549 (2001). doi:10.1086/323370
- E. Anders, N. Grevesse, Abundances of the elements - Meteoritic and solar. *Geochim. Cosmochim. Acta* **53**, 197–214 (1989). doi:10.1016/0016-7037(89)90286-X
- N. Arimoto, Y. Yoshii, Chemical and photometric properties of a galactic wind model for elliptical galaxies. *A&A* **173**, 23–38 (1987)
- D.J. Barnes, S.T. Kay, Y.M. Bahé, C. Dalla Vecchia, I.G. McCarthy, J. Schaye, R.G. Bower, A. Jenkins, P.A. Thomas, M. Schaller, R.A. Crain, T. Theuns, S.D.M. White, The Cluster-EAGLE project: global properties of simulated clusters with resolved galaxies. *MNRAS* **471**, 1088–1106 (2017). doi:10.1093/mnras/stx1647
- D.J. Barnes, M. Vogelsberger, R. Kannan, F. Marinacci, R. Weinberger, V. Springel, P. Torrey, A. Pillepich, D. Nelson, R. Pakmor, J. Naiman, L. Hernquist, M. McDonald, A census of cool-core galaxy clusters in IllustrisTNG. *MNRAS* **481**, 1809–1831 (2018). doi:10.1093/mnras/sty2078
- N. Bastian, K.R. Covey, M.R. Meyer, A Universal Stellar Initial Mass Function? A Critical Look at Variations. *ARA&A* **48**, 339–389 (2010). doi:10.1146/annurev-astro-082708-101642
- W.H. Baumgartner, M. Loewenstein, D.J. Horner, R.F. Mushotzky, Intermediate-Element Abundances in Galaxy Clusters. *ApJ* **620**, 680–696 (2005). doi:10.1086/427158
- M. Bernardi, R.K. Sheth, J.-L. Fischer, A. Meert, K.-H. Chae, H. Dominguez-Sanchez, M. Huertas-Company, F. Shankar, V. Vikram, Stellar mass functions and implications for a variable IMF. *MNRAS* **475**, 757–771 (2018). doi:10.1093/mnras/stx3171
- V. Biffi, K. Dolag, H. Böhringer, G. Lemson, Observing simulated galaxy clusters with PHOX: a novel X-ray photon simulator. *MNRAS* **420**, 3545–3556 (2012). doi:10.1111/j.1365-2966.2011.20278.x
- V. Biffi, S. Planelles, S. Borgani, D. Fabjan, E. Rasia, G. Murante, L. Tornatore, K. Dolag, G.L. Granato, M. Gaspari, A.M. Beck, The history of chemical enrichment in the intracluster medium from cosmological simulations. *MNRAS* **468**, 531–548 (2017). doi:10.1093/mnras/stx444
- V. Biffi, S. Planelles, S. Borgani, E. Rasia, G. Murante, D. Fabjan, M. Gaspari, The origin of ICM enrichment in the outskirts of present-day galaxy clusters from cosmological hydrodynamical simulations. *MNRAS* (2018). doi:10.1093/mnras/sty363
- H. Böhringer, N. Werner, X-ray spectroscopy of galaxy clusters: studying astrophysical processes in the largest celestial laboratories. *A&A Rev.* **18**, 127–196 (2010). doi:10.1007/s00159-009-0023-3
- S. Borgani, A. Kravtsov, Cosmological Simulations of Galaxy Clusters. *Advanced Science Letters* **4**, 204–227 (2011). doi:10.1166/asl.2011.1209
- S. Borgani, D. Fabjan, L. Tornatore, S. Schindler, K. Dolag, A. Diaferio, The Chemical Enrichment of the ICM from Hydrodynamical Simulations. *Space Sci. Rev.* **134**, 379–403 (2008). doi:10.1007/s11214-008-9322-7
- G. Chabrier, Galactic Stellar and Substellar Initial Mass Function. *PASP* **115**, 763–795 (2003). doi:10.1086/376392
- C. Chiappini, F. Matteucci, R. Gratton, The Chemical Evolution of the Galaxy: The Two-Infall Model. *ApJ* **477**, 765–780 (1997). doi:10.1086/303726
- A. Chieffi, M. Limongi, Explosive Yields of Massive Stars from $Z = 0$ to $Z = Z_{solar}$. *ApJ* **608**, 405–410 (2004). doi:10.1086/392523
- E. Churazov, M. Brüggen, C.R. Kaiser, H. Böhringer, W. Forman, Evolution of Buoyant Bubbles in M87. *ApJ* **554**, 261–273 (2001). doi:10.1086/321357
- S.A. Cora, Metal enrichment of the intracluster medium: a three-dimensional picture of chemical and dynamical properties. *MNRAS* **368**, 1540–1560 (2006). doi:10.1111/j.1365-2966.2006.10271.x
- S.A. Cora, L. Tornatore, P. Tozzi, K. Dolag, On the dynamical origin of the ICM metallicity evolution. *MNRAS* **386**, 96–104 (2008). doi:10.1111/j.1365-2966.2008.13068.x
- E. Cucchetti, E. Pointecouteau, P. Peille, N. Clerc, E. Rasia, V. Biffi, S. Borgani, L. Torna-

- tore, K. Dolag, M. Roncarelli, M. Gaspari, S. Ettori, E. Bulbul, T. Dauser, J. Wilms, F. Pajot, D. Barret, Athena X-IFU synthetic observations of galaxy clusters to probe the chemical enrichment of the Universe. ArXiv e-prints (2018)
- A.C. da Silva, A. Catalano, L. Montier, E. Pointecouteau, J. Lanoux, M. Giard, The impact of dust on the scaling properties of galaxy clusters. *MNRAS* **396**, 849–859 (2009). doi:10.1111/j.1365-2966.2009.14526.x
- R. Davé, B.D. Oppenheimer, S. Sivanandam, Enrichment and pre-heating in intra-group gas from galactic outflows. *MNRAS* **391**, 110–123 (2008). doi:10.1111/j.1365-2966.2008.13906.x
- S. De Grandi, S. Molendi, Metallicity Gradients in X-Ray Clusters of Galaxies. *ApJ* **551**, 153–159 (2001). doi:10.1086/320098
- S. De Grandi, S. Ettori, M. Longhetti, S. Molendi, On the iron content in rich nearby clusters of galaxies. *A&A* **419**, 7–18 (2004). doi:10.1051/0004-6361:20034228
- G. De Lucia, G. Kauffmann, S.D.M. White, Chemical enrichment of the intracluster and intergalactic medium in a hierarchical galaxy formation model. *MNRAS* **349**, 1101–1116 (2004). doi:10.1111/j.1365-2966.2004.07584.x
- J. de Plaa, The origin of the chemical elements in cluster cores. *Astronomische Nachrichten* **334**, 416 (2013). doi:10.1002/asna.201211870
- J. de Plaa, N. Werner, J.A.M. Bleeker, J. Vink, J.S. Kaastra, M. Méndez, Constraining supernova models using the hot gas in clusters of galaxies. *A&A* **465**, 345–355 (2007). doi:10.1051/0004-6361:20066382
- J. de Plaa, J.S. Kaastra, N. Werner, C. Pinto, P. Kosec, Y.-Y. Zhang, F. Mernier, L. Lovisari, H. Akamatsu, G. Schellenberger, F. Hofmann, T.H. Reiprich, A. Finoguenov, J. Ahoranta, J.S. Sanders, A.C. Fabian, O. Pols, A. Simionescu, J. Vink, H. Böhringer, CHEERS: The chemical evolution RGS sample. *A&A* **607**, 98 (2017). doi:10.1051/0004-6361/201629926
- T. Di Matteo, V. Springel, L. Hernquist, Energy input from quasars regulates the growth and activity of black holes and their host galaxies. *Nature* **433**, 604–607 (2005). doi:10.1038/nature03335
- C.L. Doherty, P. Gil-Pons, H.H.B. Lau, J.C. Lattanzio, L. Siess, Super and massive AGB stars - II. Nucleosynthesis and yields - $Z = 0.02, 0.008$ and 0.004 . *MNRAS* **437**, 195–214 (2014). doi:10.1093/mnras/stt1877
- K. Dolag, E. Mevius, R.-S. Remus, Distribution and Evolution of Metals in the Magneticum Simulations. *Galaxies* **5**, 35 (2017). doi:10.3390/galaxies5030035
- W. Domainko, M. Mair, W. Kapferer, E. van Kampen, T. Kronberger, S. Schindler, S. Kimeswenger, M. Ruffert, O.E. Mangete, Enrichment of the ICM of galaxy clusters due to ram-pressure stripping. *A&A* **452**, 795–802 (2006). doi:10.1051/0004-6361:20053921
- Y. Dubois, J. Devriendt, R. Teyssier, A. Slyz, How active galactic nucleus feedback and metal cooling shape cluster entropy profiles. *MNRAS* **417**, 1853–1870 (2011). doi:10.1111/j.1365-2966.2011.19381.x
- S. Ettori, A. Baldi, I. Balestra, F. Gastaldello, S. Molendi, P. Tozzi, The evolution of the spatially resolved metal abundance in galaxy clusters up to $z = 1.4$. *A&A* **578**, 46 (2015). doi:10.1051/0004-6361/201425470
- A.C. Fabian, Cooling Flows in Clusters of Galaxies. *ARA&A* **32**, 277–318 (1994). doi:10.1146/annurev.aa.32.090194.001425
- D. Fabjan, L. Tornatore, S. Borgani, A. Saro, K. Dolag, Evolution of the metal content of the intracluster medium with hydrodynamical simulations. *MNRAS* **386**, 1265–1273 (2008). doi:10.1111/j.1365-2966.2008.13122.x
- D. Fabjan, S. Borgani, L. Tornatore, A. Saro, G. Murante, K. Dolag, Simulating the effect of active galactic nuclei feedback on the metal enrichment of galaxy clusters. *MNRAS* **401**, 1670–1690 (2010). doi:10.1111/j.1365-2966.2009.15794.x
- Y. Fujita, N. Tawa, K. Hayashida, M. Takizawa, H. Matsumoto, N. Okabe, T.H. Reiprich, High Metallicity of the X-Ray Gas Up to the Virial Radius of a Binary Cluster of Galaxies: Evidence of Galactic Superwinds at High-Redshift. *PASJ* **60**, 343–349 (2008). doi:10.1093/pasj/60.sp1.S343
- Y. Fukazawa, K. Makishima, T. Tamura, H. Ezawa, H. Xu, Y. Ikebe, K. Kikuchi, T. Ohashi, ASCA Measurements of Silicon and Iron Abundances in the Intracluster Medium. *PASJ* **50**, 187–193 (1998). doi:10.1093/pasj/50.1.187

- A. Gardini, E. Rasia, P. Mazzotta, G. Tormen, S. De Grandi, L. Moscardini, Simulating Chandra observations of galaxy clusters. *MNRAS* **351**, 505–514 (2004). doi:10.1111/j.1365-2966.2004.07800.x
- E. Gjero, G.L. Granato, G. Murante, C. Ragone-Figueroa, L. Tornatore, S. Borgani, Dust Evolution in Galaxy Cluster Simulations. *ArXiv e-prints* (2018)
- G.L. Granato, C. Ragone-Figueroa, R. Domínguez-Tenreiro, A. Obreja, S. Borgani, G. De Lucia, G. Murante, The early phases of galaxy clusters formation in IR: coupling hydrodynamical simulations with GRASIL-3D. *MNRAS* **450**, 1320–1332 (2015). doi:10.1093/mnras/stv676
- T.H. Greif, S.C.O. Glover, V. Bromm, R.S. Klessen, Chemical mixing in smoothed particle hydrodynamics simulations. *MNRAS* **392**, 1381–1387 (2009). doi:10.1111/j.1365-2966.2008.14169.x
- A. Gupta, T. Yuan, P. Torrey, M. Vogelsberger, D. Martizzi, K.-V.H. Tran, L.J. Kewley, F. Marinacci, D. Nelson, A. Pillepich, L. Hernquist, S. Genel, V. Springel, Chemical pre-processing of cluster galaxies over the past 10 billion years in the IllustrisTNG simulations. *MNRAS* (2018). doi:10.1093/mnrasl/sly037
- O. Hahn, D. Martizzi, H.-Y. Wu, A.E. Evrard, R. Teyssier, R.H. Wechsler, Rhapsody-G simulations I: the cool cores, hot gas and stellar content of massive galaxy clusters. *ArXiv e-prints* (2015)
- S. Heinz, M. Brüggen, XIM: A virtual X-ray observatory for hydrodynamic simulations. *ArXiv e-prints* (2009)
- Hitomi Collaboration, F. Aharonian, H. Akamatsu, F. Akimoto, S.W. Allen, L. Angelini, M. Audard, H. Awaki, M. Axelsson, A. Bamba, M.W. Bautz, R. Blandford, L.W. Brenneman, G.V. Brown, E. Bulbul, E.M. Cackett, M. Chernyakova, M.P. Chiao, P.S. Coppi, E. Costantini, J. de Plaa, C.P. de Vries, J.-W. den Herder, C. Done, T. Dotani, K. Ebisawa, M.E. Eckart, T. Enoto, Y. Ezoe, A.C. Fabian, C. Ferrigno, A.R. Foster, R. Fujimoto, Y. Fukazawa, A. Furuzawa, M. Galeazzi, L.C. Gallo, P. Gandhi, M. Giustini, A. Goldwurm, L. Gu, M. Guainazzi, Y. Haba, K. Hagino, K. Hamaguchi, I.M. Harrus, I. Hatsukade, K. Hayashi, T. Hayashi, K. Hayashida, N. Hell, J.S. Hiraga, A. Hornschemeier, A. Hoshino, J.P. Hughes, Y. Ichinohe, R. Iizuka, H. Inoue, Y. Inoue, M. Ishida, K. Ishikawa, Y. Ishisaki, M. Iwai, J. Kaastra, T. Kallman, T. Kamae, J. Kataoka, S. Katsuda, N. Kawai, R.L. Kelley, C.A. Kilbourne, T. Kitaguchi, S. Kitamoto, T. Kitayama, T. Kohmura, M. Kokubun, K. Koyama, S. Koyama, P. Kretschmar, H.A. Krimm, A. Kubota, H. Kunieda, P. Laurent, S.-H. Lee, M.A. Leutenegger, O. Limousin, M. Loewenstein, K.S. Long, D. Lumb, G. Madejski, Y. Maeda, D. Maier, K. Makishima, M. Markevitch, H. Matsumoto, K. Matsushita, D. McCammon, B.R. McNamara, M. Mehdipour, E.D. Miller, J.M. Miller, S. Mineshige, K. Mitsuda, I. Mitsuishi, T. Miyazawa, T. Mizuno, H. Mori, K. Mori, K. Mukai, H. Murakami, R.F. Mushotzky, T. Nakagawa, H. Nakajima, T. Nakamori, S. Nakashima, K. Nakazawa, K.K. Nobukawa, M. Nobukawa, H. Noda, H. Odaka, T. Ohashi, M. Ohno, T. Okajima, N. Ota, M. Ozaki, F. Paerels, S. Paltani, R. Petre, C. Pinto, F.S. Porter, K. Pottschmidt, C.S. Reynolds, S. Safi-Harb, S. Saito, K. Sakai, T. Sasaki, G. Sato, K. Sato, R. Sato, M. Sawada, N. Schartel, P.J. Serlemitsos, H. Seta, M. Shidatsu, A. Simionescu, R.K. Smith, Y. Soong, L. Stawarz, Y. Sugawara, S. Sugita, A. Szymkowiak, H. Tajima, H. Takahashi, T. Takahashi, S. Takeda, Y. Takei, T. Tamagawa, T. Tamura, T. Tanaka, Y. Tanaka, Y.T. Tanaka, M.S. Tashiro, Y. Tawara, Y. Terada, Y. Terashima, F. Tombesi, H. Tomida, Y. Tsuboi, M. Tsujimoto, H. Tsunemi, T.G. Tsuru, H. Uchida, H. Uchiyama, Y. Uchiyama, S. Ueda, Y. Ueda, S. Uno, C.M. Urry, E. Ursino, S. Watanabe, N. Werner, D.R. Wilkins, B.J. Williams, S. Yamada, H. Yamaguchi, K. Yamaoka, N.Y. Yamasaki, M. Yamauchi, S. Yamauchi, T. Yaqoob, Y. Yatsu, D. Yonetoku, I. Zhuravleva, A. Zoghbi, A.J.J. Raassen, Atomic data and spectral modeling constraints from high-resolution X-ray observations of the Perseus cluster with Hitomi. *PASJ* **70**, 12 (2018). doi:10.1093/pasj/psx156
- D.S. Hudson, R. Mittal, T.H. Reiprich, P.E.J. Nulsen, H. Andernach, C.L. Sarazin, What is a cool-core cluster? a detailed analysis of the cores of the X-ray flux-limited HIFLUGCS cluster sample. *A&A* **513**, 37 (2010). doi:10.1051/0004-6361/200912377
- K. Iwamoto, F. Brachwitz, K. Nomoto, N. Kishimoto, H. Umeda, W.R. Hix, F.-K. Thielemann, Nucleosynthesis in Chandrasekhar Mass Models for Type IA Supernovae and Constraints on Progenitor Systems and Burning-Front Propagation. *ApJS* **125**, 439–

- 462 (1999). doi:10.1086/313278
- W. Kapferer, T. Kronberger, J. Weratschnig, S. Schindler, W. Domainko, E. van Kampen, S. Kimeswenger, M. Mair, M. Ruffert, Metal enrichment of the intra-cluster medium over a Hubble time for merging and relaxed galaxy clusters. *A&A* **466**, 813–821 (2007). doi:10.1051/0004-6361:20066804
- A. Karakas, J.C. Lattanzio, Stellar Models and Yields of Asymptotic Giant Branch Stars. *PASA* **24**, 103–117 (2007). doi:10.1071/AS07021
- A.I. Karakas, Updated stellar yields from asymptotic giant branch models. *MNRAS* **403**, 1413–1425 (2010). doi:10.1111/j.1365-2966.2009.16198.x
- A.I. Karakas, J.C. Lattanzio, The Dawes Review 2: Nucleosynthesis and Stellar Yields of Low- and Intermediate-Mass Single Stars. *PASA* **31**, 030 (2014). doi:10.1017/pasa.2014.21
- N. Katz, Dissipational galaxy formation. II - Effects of star formation. *ApJ* **391**, 502–517 (1992). doi:10.1086/171366
- D. Kawata, B.K. Gibson, GCD+: a new chemodynamical approach to modelling supernovae and chemical enrichment in elliptical galaxies. *MNRAS* **340**, 908–922 (2003). doi:10.1046/j.1365-8711.2003.06356.x
- D. Kawata, B.K. Gibson, D.J. Barnes, R.J.J. Grand, A. Rahimi, Numerical simulations of bubble-induced star formation in dwarf irregular galaxies with a novel stellar feedback scheme. *MNRAS* **438**, 1208–1222 (2014). doi:10.1093/mnras/stt2267
- C.C. Kirkpatrick, B.R. McNamara, Hot outflows in galaxy clusters. *MNRAS* **452**, 4361–4376 (2015). doi:10.1093/mnras/stv1574
- C. Kobayashi, H. Umeda, K. Nomoto, N. Tominaga, T. Ohkubo, Galactic Chemical Evolution: Carbon through Zinc. *ApJ* **653**, 1145–1171 (2006). doi:10.1086/508914
- P. Kroupa, On the variation of the initial mass function. *MNRAS* **322**, 231–246 (2001). doi:10.1046/j.1365-8711.2001.04022.x
- P. Kroupa, C.A. Tout, G. Gilmore, The distribution of low-mass stars in the Galactic disc. *MNRAS* **262**, 545–587 (1993). doi:10.1093/mnras/262.3.545
- A. Leccardi, S. Molendi, Radial metallicity profiles for a large sample of galaxy clusters observed with XMM-Newton. *A&A* **487**, 461–466 (2008). doi:10.1051/0004-6361:200810113
- A. Leccardi, M. Rossetti, S. Molendi, Thermo-dynamic and chemical properties of the intra-cluster medium. *A&A* **510**, 82 (2010). doi:10.1051/0004-6361/200913094
- C. Lia, L. Portinari, G. Carraro, Star formation and chemical evolution in smoothed particle hydrodynamics simulations: a statistical approach. *MNRAS* **330**, 821–836 (2002). doi:10.1046/j.1365-8711.2002.05118.x
- L. Liang, F. Durier, A. Babul, R. Davé, B.D. Oppenheimer, N. Katz, M. Fardal, T. Quinn, The growth and enrichment of intragroup gas. *MNRAS* **456**, 4266–4290 (2016). doi:10.1093/mnras/stv2840
- A. Maeder, G. Meynet, Grids of evolutionary models from 0.85 to 120 solar masses - Observational tests and the mass limits. *A&A* **210**, 155–173 (1989)
- U. Maio, K. Dolag, B. Ciardi, L. Tornatore, Metal and molecule cooling in simulations of structure formation. *MNRAS* **379**, 963–973 (2007). doi:10.1111/j.1365-2966.2007.12016.x
- A.B. Mantz, S.W. Allen, R.G. Morris, A. Simionescu, O. Urban, N. Werner, I. Zhuravleva, The metallicity of the intracluster medium over cosmic time: further evidence for early enrichment. *MNRAS* **472**, 2877–2888 (2017). doi:10.1093/mnras/stx2200
- P. Marigo, Chemical yields from low- and intermediate-mass stars: Model predictions and basic observational constraints. *A&A* **370**, 194–217 (2001). doi:10.1051/0004-6361:20000247
- D. Martizzi, O. Hahn, H.-Y. Wu, A.E. Evrard, R. Teyssier, R.H. Wechsler, RHAPSODY-G simulations - II. Baryonic growth and metal enrichment in massive galaxy clusters. *MNRAS* **459**, 4408–4427 (2016). doi:10.1093/mnras/stw897
- K. Matsushita, T. Sato, E. Sakuma, K. Sato, Distribution of Si, Fe, and Ni in the Intracluster Medium of the Coma Cluster. *PASJ* **65**, 10 (2013a). doi:10.1093/pasj/65.1.10
- K. Matsushita, E. Sakuma, T. Sasaki, K. Sato, A. Simionescu, Metal-mass-to-light Ratios of the Perseus Cluster Out to the Virial Radius. *ApJ* **764**, 147 (2013b). doi:10.1088/0004-637X/764/2/147

- F. Matteucci, *The Chemical Evolution of the Galaxy* 2003
- F. Matteucci, B.K. Gibson, Chemical abundances in clusters of galaxies. *A&A* **304**, 11 (1995)
- B.J. Maughan, C. Jones, W. Forman, L. Van Speybroeck, Images, Structural Properties, and Metal Abundances of Galaxy Clusters Observed with Chandra ACIS-I at 0.1 z \leq 1.3. *ApJS* **174**, 117–135 (2008). doi:10.1086/521225
- P. Mazzotta, E. Rasia, L. Moscardini, G. Tormen, Comparing the temperatures of galaxy clusters from hydrodynamical N-body simulations to Chandra and XMM-Newton observations. *MNRAS* **354**, 10–24 (2004). doi:10.1111/j.1365-2966.2004.08167.x
- I.G. McCarthy, J. Schaye, R.G. Bower, T.J. Ponman, C.M. Booth, C. Dalla Vecchia, V. Springel, Gas expulsion by quasar-driven winds as a solution to the overcooling problem in galaxy groups and clusters. *MNRAS* **412**, 1965–1984 (2011). doi:10.1111/j.1365-2966.2010.18033.x
- M. McDonald, E. Bulbul, T. de Haan, E.D. Miller, B.A. Benson, L.E. Bleem, M. Brodwin, J.E. Carlstrom, I. Chiu, W.R. Forman, J. Hlavacek-Larrondo, G.P. Garmire, N. Gupta, J.J. Mohr, C.L. Reichardt, A. Saro, B. Stalder, A.A. Stark, J.D. Vieira, The Evolution of the Intracluster Medium Metallicity in Sunyaev Zel’dovich-selected Galaxy Clusters at 0 z \leq 1.5. *ApJ* **826**, 124 (2016). doi:10.3847/0004-637X/826/2/124
- F. Mernier, J. de Plaa, C. Pinto, J.S. Kaastra, P. Kosec, Y.-Y. Zhang, J. Mao, N. Werner, Origin of central abundances in the hot intra-cluster medium. I. Individual and average abundance ratios from XMM-Newton EPIC. *A&A* **592** (2016). doi:10.1051/0004-6361/201527824
- F. Mernier, J. de Plaa, J.S. Kaastra, Y.-Y. Zhang, H. Akamatsu, L. Gu, P. Kosec, J. Mao, C. Pinto, T.H. Reiprich, J.S. Sanders, A. Simionescu, N. Werner, Radial metal abundance profiles in the intra-cluster medium of cool-core galaxy clusters, groups, and ellipticals. *A&A* **603**, 80 (2017). doi:10.1051/0004-6361/201630075
- F. Mernier, J. de Plaa, N. Werner, J.S. Kaastra, A.J.J. Raassen, L. Gu, J. Mao, I. Urdampilleta, N. Truong, A. Simionescu, Mass-invariance of the iron enrichment in the hot haloes of massive ellipticals, groups, and clusters of galaxies. *MNRAS* **478**, 116–121 (2018). doi:10.1093/mnras/sly080
- G.E. Miller, J.M. Scalo, The initial mass function and stellar birthrate in the solar neighborhood. *ApJS* **41**, 513–547 (1979). doi:10.1086/190629
- S. Molendi, F. Pizzolato, Is the Gas in Cooling Flows Multiphase? *ApJ* **560**, 194–200 (2001). doi:10.1086/322387
- R. Moll, S. Schindler, W. Domainko, W. Kapferer, M. Mair, E. van Kampen, T. Kronberger, S. Kimeswenger, M. Ruffert, Simulations of metal enrichment in galaxy clusters by AGN outflows. *A&A* **463**, 513–518 (2007). doi:10.1051/0004-6361:20066386
- L.A. Montier, M. Giard, The importance of dust in cooling and heating the InterGalactic Medium. *A&A* **417**, 401–409 (2004). doi:10.1051/0004-6361:20034365
- M.B. Mosconi, P.B. Tissera, D.G. Lambas, S.A. Cora, Chemical evolution using smooth particle hydrodynamical cosmological simulations - I. Implementation, tests and first results. *MNRAS* **325**, 34–48 (2001). doi:10.1046/j.1365-8711.2001.04198.x
- G. Murante, P. Monaco, M. Giovalli, S. Borgani, A. Diaferio, A subresolution multiphase interstellar medium model of star formation and supernova energy feedback. *MNRAS* **405**, 1491–1512 (2010). doi:10.1111/j.1365-2966.2010.16567.x
- M. Nagashima, C.G. Lacey, C.M. Baugh, C.S. Frenk, S. Cole, The metal enrichment of the intracluster medium in hierarchical galaxy formation models. *MNRAS* **358**, 1247–1266 (2005). doi:10.1111/j.1365-2966.2005.08766.x
- J.P. Naiman, A. Pillepich, V. Springel, E. Ramirez-Ruiz, P. Torrey, M. Vogelsberger, R. Pakmor, D. Nelson, F. Marinacci, L. Hernquist, R. Weinberger, S. Genel, First results from the IllustrisTNG simulations: A tale of two elements - chemical evolution of magnesium and europium. *MNRAS* (2018). doi:10.1093/mnras/sty618
- K. Nomoto, C. Kobayashi, N. Tominaga, Nucleosynthesis in Stars and the Chemical Enrichment of Galaxies. *ARA&A* **51**, 457–509 (2013). doi:10.1146/annurev-astro-082812-140956
- K. Nomoto, K. Iwamoto, N. Nakasato, F.-K. Thielemann, F. Brachwitz, T. Tsujimoto, Y. Kubo, N. Kishimoto, Nucleosynthesis in type Ia supernovae. *Nuclear Physics A* **621**, 467–476 (1997). doi:10.1016/S0375-9474(97)00291-1

- P. Padovani, F. Matteucci, Stellar Mass Loss in Elliptical Galaxies and the Fueling of Active Galactic Nuclei. *ApJ* **416**, 26 (1993). doi:10.1086/173212
- S. Planelles, S. Borgani, D. Fabjan, M. Killevar, G. Murante, G.L. Granato, C. Ragone-Figueroa, K. Dolag, On the role of AGN feedback on the thermal and chemodynamical properties of the hot intracluster medium. *MNRAS* **438**, 195–216 (2014). doi:10.1093/mnras/stt2141
- E. Pointecouteau, A. da Silva, A. Catalano, L. Montier, J. Lanoux, M. Roncarelli, M. Giard, Simulating the impact of dust cooling on the statistical properties of the intra-cluster medium. *Advances in Space Research* **44**, 440–445 (2009). doi:10.1016/j.asr.2009.05.006
- L. Portinari, C. Chiosi, A. Bressan, Galactic chemical enrichment with new metallicity dependent stellar yields. *A&A* **334**, 505–539 (1998)
- E. Puchwein, D. Sijacki, V. Springel, Simulations of AGN Feedback in Galaxy Clusters and Groups: Impact on Gas Fractions and the L_X -T Scaling Relation. *ApJ* **687**, 53 (2008). doi:10.1086/593352
- C.M. Raiteri, M. Villata, J.F. Navarro, Simulations of Galactic chemical evolution. I. O and Fe abundances in a simple collapse model. *A&A* **315**, 105–115 (1996)
- E. Rasia, P. Mazzotta, H. Bourdin, S. Borgani, L. Tornatore, S. Ettori, K. Dolag, L. Moscardini, X-MAS2: Study Systematics on the ICM Metallicity Measurements. *ApJ* **674**, 728–741 (2008). doi:10.1086/524345
- E. Rasia, S. Borgani, G. Murante, S. Planelles, A.M. Beck, V. Biffi, C. Ragone-Figueroa, G.L. Granato, L.K. Steinborn, K. Dolag, Cool Core Clusters from Cosmological Simulations. *ApJ* **813**, 17 (2015). doi:10.1088/2041-8205/813/1/L17
- J. Rasmussen, T.J. Ponman, Temperature and abundance profiles of hot gas in galaxy groups - I. Results and statistical analysis. *MNRAS* **380**, 1554–1572 (2007). doi:10.1111/j.1365-2966.2007.12191.x
- J. Rasmussen, T.J. Ponman, Temperature and abundance profiles of hot gas in galaxy groups - II. Implications for feedback and ICM enrichment. *MNRAS* **399**, 239–263 (2009). doi:10.1111/j.1365-2966.2009.15244.x
- P. Rebusco, E. Churazov, H. Böhringer, W. Forman, Impact of stochastic gas motions on galaxy cluster abundance profiles. *MNRAS* **359**, 1041–1048 (2005). doi:10.1111/j.1365-2966.2005.08965.x
- P. Rebusco, E. Churazov, H. Böhringer, W. Forman, Effect of turbulent diffusion on iron abundance profiles. *MNRAS* **372**, 1840–1850 (2006). doi:10.1111/j.1365-2966.2006.10977.x
- D. Romano, C. Chiappini, F. Matteucci, M. Tosi, Quantifying the uncertainties of chemical evolution studies. I. Stellar lifetimes and initial mass function. *A&A* **430**, 491–505 (2005). doi:10.1051/0004-6361:20048222
- D. Romano, A.I. Karakas, M. Tosi, F. Matteucci, Quantifying the uncertainties of chemical evolution studies. II. Stellar yields. *A&A* **522**, 32 (2010a). doi:10.1051/0004-6361/201014483
- D. Romano, A.I. Karakas, M. Tosi, F. Matteucci, Quantifying the uncertainties of chemical evolution studies. II. Stellar yields. *A&A* **522**, 32 (2010b). doi:10.1051/0004-6361/201014483
- A.D. Romeo, J. Sommer-Larsen, L. Portinari, V. Antonuccio-Delogu, Simulating galaxy clusters - I. Thermal and chemical properties of the intracluster medium. *MNRAS* **371**, 548–568 (2006). doi:10.1111/j.1365-2966.2006.10735.x
- M. Rossetti, D. Eckert, B.M. Cavalleri, S. Molendi, F. Gastaldello, S. Ghizzardi, Back and forth from cool core to non-cool core: clues from radio halos. *A&A* **532**, 123 (2011). doi:10.1051/0004-6361/201117306
- E. Sakuma, N. Ota, K. Sato, T. Sato, K. Matsushita, Suzaku Observations of Metal Distributions in the Intracluster Medium of the Centaurus Cluster. *PASJ* **63**, 979–990 (2011). doi:10.1093/pasj/63.sp3.S979
- E.E. Salpeter, The Luminosity Function and Stellar Evolution. *ApJ* **121**, 161 (1955). doi:10.1086/145971
- K. Sato, K. Matsushita, Y. Ishisaki, N.Y. Yamasaki, M. Ishida, S. Sasaki, T. Ohashi, Suzaku Observations of AWM 7 Cluster of Galaxies: Temperatures, Abundances, and Bulk Motions. *PASJ* **60**, 333–342 (2008). doi:10.1093/pasj/60.sp1.S333
- C. Scannapieco, P.B. Tissera, S.D.M. White, V. Springel, Feedback and metal enrichment

- in cosmological smoothed particle hydrodynamics simulations - I. A model for chemical enrichment. *MNRAS* **364**, 552–564 (2005). doi:10.1111/j.1365-2966.2005.09574.x
- S. Schindler, A. Diaferio, Metal Enrichment Processes. *Space Sci. Rev.* **134**, 363–377 (2008). doi:10.1007/s11214-008-9321-8
- S. Schindler, W. Kapferer, W. Domainko, M. Mair, E. van Kampen, T. Kronberger, S. Kimeswenger, M. Ruffert, O. Mangete, D. Breitschwerdt, Metal enrichment processes in the intra-cluster medium. *A&A* **435**, 25–28 (2005). doi:10.1051/0004-6361:200500107
- C.J. Short, P.A. Thomas, O.E. Young, Heating and enriching the intracluster medium. *MNRAS* **428**, 1225–1247 (2013). doi:10.1093/mnras/sts107
- D. Sijacki, V. Springel, Hydrodynamical simulations of cluster formation with central AGN heating. *MNRAS* **366**, 397–416 (2006). doi:10.1111/j.1365-2966.2005.09860.x
- A. Simionescu, N. Werner, A. Finoguenov, H. Böhringer, M. Brüggen, Metal-rich multi-phase gas in M 87. AGN-driven metal transport, magnetic-field supported multi-temperature gas, and constraints on non-thermal emission observed with XMM-Newton. *A&A* **482**, 97–112 (2008). doi:10.1051/0004-6361:20078749
- A. Simionescu, N. Werner, H. Böhringer, J.S. Kaastra, A. Finoguenov, M. Brüggen, P.E.J. Nulsen, Chemical enrichment in the cluster of galaxies Hydra A. *A&A* **493**, 409–424 (2009). doi:10.1051/0004-6361:200810225
- A. Simionescu, N. Werner, O. Urban, S.W. Allen, Y. Ichinohe, I. Zhuravleva, A Uniform Contribution of Core-collapse and Type Ia Supernovae to the Chemical Enrichment Pattern in the Outskirts of the Virgo Cluster. *ApJ* **811**, 25 (2015). doi:10.1088/2041-8205/811/2/L25
- J. Sommer-Larsen, M. Götz, L. Portinari, Galaxy Formation: Cold Dark Matter, Feedback, and the Hubble Sequence. *ApJ* **596**, 47–66 (2003). doi:10.1086/377685
- V. Springel, The cosmological simulation code GADGET-2. *MNRAS* **364**, 1105–1134 (2005). doi:10.1111/j.1365-2966.2005.09655.x
- V. Springel, E pur si muove: Galilean-invariant cosmological hydrodynamical simulations on a moving mesh. *MNRAS* **401**, 791–851 (2010). doi:10.1111/j.1365-2966.2009.15715.x
- V. Springel, L. Hernquist, Cosmological smoothed particle hydrodynamics simulations: a hybrid multiphase model for star formation. *MNRAS* **339**, 289–311 (2003). doi:10.1046/j.1365-8711.2003.06206.x
- V. Springel, T. Di Matteo, L. Hernquist, Black Holes in Galaxy Mergers: The Formation of Red Elliptical Galaxies. *ApJ* **620**, 79–82 (2005). doi:10.1086/428772
- M. Steinmetz, E. Mueller, The formation of disk galaxies in a cosmological context: Populations, metallicities and metallicity gradients. *A&A* **281**, 97–100 (1994)
- M. Sun, Hot gas in galaxy groups: recent observations. *New Journal of Physics* **14**(4), 045004 (2012). doi:10.1088/1367-2630/14/4/045004
- R.S. Sutherland, M.A. Dopita, Cooling functions for low-density astrophysical plasmas. *ApJS* **88**, 253–327 (1993). doi:10.1086/191823
- R. Teyssier, B. Moore, D. Martizzi, Y. Dubois, L. Mayer, Mass distribution in galaxy clusters: the role of Active Galactic Nuclei feedback. *MNRAS* **414**, 195–208 (2011). doi:10.1111/j.1365-2966.2011.18399.x
- F.-K. Thielemann, D. Argast, F. Brachwitz, W.R. Hix, P. Höflich, M. Liebendörfer, G. Martinez-Pinedo, A. Mezzacappa, K. Nomoto, I. Panov, Supernova Nucleosynthesis and Galactic Evolution, in *From Twilight to Highlight: The Physics of Supernovae*, ed. by W. Hillebrandt, B. Leibundgut, 2003, p. 331
- L. Tornatore, S. Borgani, F. Matteucci, S. Recchi, P. Tozzi, Simulating the metal enrichment of the intracluster medium. *MNRAS* **349**, 19–24 (2004). doi:10.1111/j.1365-2966.2004.07689.x
- L. Tornatore, S. Borgani, K. Dolag, F. Matteucci, Chemical enrichment of galaxy clusters from hydrodynamical simulations. *MNRAS* **382**, 1050–1072 (2007). doi:10.1111/j.1365-2966.2007.12070.x
- C. Travaglio, W. Hillebrandt, M. Reinecke, F.-K. Thielemann, Nucleosynthesis in multi-dimensional SN Ia explosions. *A&A* **425**, 1029–1040 (2004). doi:10.1051/0004-6361:20041108
- N. Truong, E. Rasia, V. Biffi, F. Mernier, N. Werner, M. Gaspari, S. Borgani, S. Planelles, D. Fabjan, G. Murante, Mass-Metallicity Relation from Cosmological Hydrodynamical Simulations and X-ray Observations of Galaxy Groups and Clusters. *ArXiv e-prints*

- (2018)
- O. Urban, N. Werner, S.W. Allen, A. Simionescu, A. Mantz, A uniform metallicity in the outskirts of massive, nearby galaxy clusters. *MNRAS* **470**, 4583–4599 (2017). doi:10.1093/mnras/stx1542
- R. Valdarnini, Iron abundances and heating of the intracluster medium in hydrodynamical simulations of galaxy clusters. *MNRAS* **339**, 1117–1134 (2003). doi:10.1046/j.1365-8711.2003.06163.x
- L.B. van den Hoek, M.A.T. Groenewegen, New theoretical yields of intermediate mass stars. *A&AS* **123**, 305–328 (1997). doi:10.1051/aas:1997162
- A. Vikhlinin, M. Markevitch, S.S. Murray, C. Jones, W. Forman, L. Van Speybroeck, Chandra Temperature Profiles for a Sample of Nearby Relaxed Galaxy Clusters. *ApJ* **628**, 655–672 (2005). doi:10.1086/431142
- M. Vogelsberger, F. Marinacci, P. Torrey, S. Genel, V. Springel, R. Weinberger, R. Pakmor, L. Hernquist, J. Naiman, A. Pillepich, D. Nelson, The uniformity and time-invariance of the intra-cluster metal distribution in galaxy clusters from the IllustrisTNG simulations. *MNRAS* **474**, 2073–2093 (2018). doi:10.1093/mnras/stx2955
- N. Werner, F. Durret, T. Ohashi, S. Schindler, R.P.C. Wiersma, Observations of Metals in the Intra-Cluster Medium. *Space Sci. Rev.* **134**, 337–362 (2008). doi:10.1007/s11214-008-9320-9
- N. Werner, O. Urban, A. Simionescu, S.W. Allen, A uniform metal distribution in the intergalactic medium of the Perseus cluster of galaxies. *Nature* **502**, 656–658 (2013). doi:10.1038/nature12646
- R.P.C. Wiersma, J. Schaye, B.D. Smith, The effect of photoionization on the cooling rates of enriched, astrophysical plasmas. *MNRAS* **393**, 99–107 (2009a). doi:10.1111/j.1365-2966.2008.14191.x
- R.P.C. Wiersma, J. Schaye, T. Theuns, C. Dalla Vecchia, L. Tornatore, Chemical enrichment in cosmological, smoothed particle hydrodynamics simulations. *MNRAS* **399**, 574–600 (2009b). doi:10.1111/j.1365-2966.2009.15331.x
- D. Williamson, H. Martel, D. Kawata, Metal Diffusion in Smoothed Particle Hydrodynamics Simulations of Dwarf Galaxies. *ApJ* **822**, 91 (2016). doi:10.3847/0004-637X/822/2/91
- S.E. Woosley, T.A. Weaver, The Evolution and Explosion of Massive Stars. II. Explosive Hydrodynamics and Nucleosynthesis. *ApJS* **101**, 181 (1995). doi:10.1086/192237
- R.M. Yates, P.A. Thomas, B.M.B. Henriques, Iron in galaxy groups and clusters: confronting galaxy evolution models with a newly homogenized data set. *MNRAS* **464**, 3169–3193 (2017). doi:10.1093/mnras/stw2361
- J.A. ZuHone, V. Biffi, E.J. Hallman, S.W. Randall, A.R. Foster, C. Schmid, Simulating X-ray Observations with Python. *ArXiv e-prints* (2014)